Growth and maturity of Longnose Skates (*Raja rhina)* along the North American West Coast

Morgan Brittany Arrington

A thesis

submitted in partial fulfillment of the

requirements for the degree of

Master of Science

University of Washington

2020

Committee:

Timothy E. Essington

Thomas Helser

Mary Elizabeth Matta

André E. Punt

Program Authorized to Offer Degree:

Aquatic and Fishery Sciences

University of Washington

Abstract

Growth and maturity of Longnose Skates (*Raja rhina)* along the North American West Coast

Morgan Brittany Arrington

Chair of the Supervisory Committee:
Timothy Essington
Aquatic and Fishery Sciences

Information on the growth and maturation of exploited fishes is important for assessing and managing fish populations. These life history processes commonly vary spatially and temporarily in marine fishes due to environmental and ecological factors, which can have implications for management. However, acquiring biological information on marine fishes on large spatial and temporal scales can be expensive and time consuming. This is especially true for elasmobranchs because elasmobranchs do not possess otoliths, which are commonly used for age-estimation in teleost fishes. Instead, alternative methods are used which are time intensive and often have reduced precision. The Longnose Skate is a species of elasmobranch commonly caught as bycatch in groundfish fisheries along the North American West Coast. Individuals are acted upon by variable environmental and ecological conditions along their large range that may impact growth and maturity. The first chapter of this thesis explores spatial variability in the size-at-age and size-

at-maturation of Longnose Skates along their geographic range from the Gulf of Alaska to Southern California. We found that growth and maturity varied between the regions (1) Western and Central Gulf of Alaska, (2) Eastern Gulf of Alaska/ British Columbia, and (3) the U.S. West Coast along a latitudinal cline. The second chapter explores the application of an emerging technology called Fourier transform near infrared spectroscopy (FT-NIRS) to more rapidly estimate ages for Longnose Skates. We found that FT-NIRS technology was able to predict Longnose Skate ages within 1.45 years of the traditionally generated age 68% of the time (R^2 = 0.87, RMSE = 1.45 years) in approximately $1/8^{th}$ of the time. These findings suggest that life history parameters used in stock assessments, such as size-at-age and maturation-at-size, do vary spatially. Additionally, efficiencies can be gained by utilizing FT-NIRS technology to estimate ages for Longnose Skates which may make it possible to increase the quantity and temporal resolution of age data that is incorporated into stock assessments.

TABLE OF CONTENTS

LIST OF FIGURES

LIST OF TABLES

ACKNOWLEDGEMENTS

There are many people I would like to thank for the ways they contributed to this thesis and to my development as a scientist. First, thank you to my wonderful committee for your guidance in my endeavor to attain a graduate degree. My advisor, Tim Essington, thank you for your steadfast and encouraging mentorship. Your patience and dedication were critical to my success, and your positivity and infectious laugh kept me smiling throughout. Beth Matta, thank you for being a wonderful role model and advocate. Your enthusiasm for science and attention to detail inspired me, and your kindness encouraged me when I needed it most. Many thanks to Tom Helser - your active listening and thoughtful questions were vital to improving the quality of my research. I thank André Punt for always making me feel welcome and like my research mattered. I appreciate your hard questions and your gift for asking them in a way that inspires growth and learning.

While pursuing a graduate degree, I was supported by an entire community both inside and outside of my academic life. To the Essington Lab (and Friends!), it has been wonderful to be a part of this amazing group and my thanks goes out to each one of you. You model the best of science and of people and you each inspire me in your own unique way. Thank you to my fabulous interns Emma Evans and Melinda Carr for all of your diligence and hard work - I look forward to remaining friends and following your careers. I am also so thankful to the wider SAFS community including our wonderful administration. I am leaving with a degree, but also life-long friends. To my friends and family – you supported me in my personal life and made it possible for me to pursue my passion. For this I will be forever thankful. Members of King County Search Dogs, it has been such a privilege to be a part of this amazing group of motivated and passionate individuals. It kept me balanced throughout my time in graduate school and gave my life a deeper meaning. Lastly, thank you to my dog Roux for being my biggest fan and always thinking I am #1.

Thank you to my funding sources for investing in my research and career development. These include the National Oceanic and Atmospheric Administration (NOAA) Improving Stock Assessment grant and the School of Aquatic and Fishery Sciences.

Chapter 1. SPATIAL VARIABILITY IN THE GROWTH AND MATURITY OF LONGNOSE SKATES (*RAJA RHINA)* ALONG THE NORTH AMERICAN WEST COAST

1.1 ABSTRACT

Biological information regarding growth and reproduction is important for predicting the resiliency of a species to exploitation. Intraspecific variation in these life processes is prevalent in the natural world and can have implications for the appropriate spatial scale for resource management. The Longnose Skate (*Raja rhina*) is a species of elasmobranch commonly caught as bycatch in groundfish fisheries from the Gulf of Alaska to Southern California. Several studies on the growth and maturity of Longnose Skates have been conducted in different regions producing conflicting estimates of size-at-age and size-at-maturity. It is unknown whether these differences among studies indicate spatial variability in growth and maturity or are an artifact of different methodologies among agencies. Here, we evaluate variability in growth and maturity along the Longnose Skate's geographic range from the Gulf of Alaska to Southern California at broad and fine spatial scales using standardized age determination methodology. We explore variability in growth by fitting growth models with different combinations of stock-wide versus area-specific parameter estimates. We explored variability in size-at-maturity using logistic regression with area as a random effect. Growth varied between the large regions (1) western and central Gulf of Alaska, (2) Eastern Gulf of Alaska/ British Columbia, and (3) the U.S. West Coast based on the coefficient of anabolism (q) along a latitudinal cline. At a comparable age (14 years) Longnose Skates were on average larger in region 1 (120 ± 0.59 cm) than region 2 (108 ± 0.72) and region 3 (102 ± 2.67 cm). Longnose Skates also matured at larger sizes in region 1 relative to region 2 and

region 3 (region 1 = M: 99 cm [94.71, 103.35], F: 112 cm [108.32, 115.37], region 2 = M: 85 cm [76.33, 95.41], F: 102 cm [92.56, 109.74]; region 3 = M: 74 cm [69.49, 79.02], F: 92.52 cm [87.48, 98.75]). The results of this study suggest that regional differences in the growth of Longnose Skates are driven by variability in bottom-up processes such as food availability. Additionally, these findings illustrate that life history parameters used in stock assessments, such as size-at-age and maturation-at-size, should be based on region-specific estimates.

1.2 INTRODUCTION

Understanding intraspecific spatial variability in the life history of exploited fishes can lend insight into ecological processes and inform natural resource management decisions. Growth and maturity are critical life processes that govern fish population dynamics. Growth directly impacts population production, through direct effects on biomass accrual (Stawitz and Essington 2019) and also through indirect effects on age-at-maturity (Stearns 1992), fecundity (Fahy and Spieler 2007; Green 2008), size-dependent mortality (Mangel 2017), and vulnerability to fishing gear. At the same time, growth rate is governed by local environmental and ecological conditions (Shelton and Mangel 2012, Matta et al. 2018), density dependence (Lorenzen and Enberg 2001), and genetics (Conover et al. 1997, Roff 1991).

Differences in growth and maturity can exist over multiple spatial scales due to a variety of environmental factors, and can also suggest differences in physio-chemical environment, ecosystem productivity, or food web structures. For example, differences in growth rate of marine fish has been correlated with temperature and prey availability as well as ecosystem productivity and inter-specific competition (Reum et al. 2013, Mello and Rose 2005, Matta et al. 2018, Matta et al. 2020). Many species demonstrate phenotypic plasticity in maturation, whereby slower-growing fish mature at older ages than faster-growing fish (Morita and Morita 2002). This is due

to trade-offs between reallocating energy to maturing earlier and at smaller sizes to extend the reproductive period versus maturing later and larger to increase body size and therefore fecundity (Stearns 1992). Variability in growth is especially common in species with wide latitudinal ranges; individuals within a species are typically larger at higher latitudes, which has implications for the timing of maturity (Atkinson 1997, Morita and Morita 2002).

Age and maturity data are also commonly used to estimate population status in stock assessments that inform resource management decisions. Accurate age estimates are important because error in size-at-age data can affect projections of stock status (Maunder et al. 2015). Campana (2001) reviewed numerous cases where inaccurate age estimates ultimately resulted in the overexploitation of a species. Similarly, if size-at-age estimates are uniformly applied to a stock when spatial variation exists, stock productivity may be underestimated in some regions and overestimated in others. This can lead to both under and over-utilization of a resource (Tuckey et al. 2007). It is therefore important to evaluate spatial variation in size-at-age to inform appropriate management decisions.

Longnose Skates (*Raja rhina*) are a species of elasmobranch with a wide geographic range from Alaska to Baja, California, and therefore individuals experience widely variable conditions that may impact growth and maturity. Additionally, disagreement in results among previous growth and maturity studies suggests potential for spatial variability. Growth and the timing of maturation has been estimated separately for Longnose Skates in the Gulf of Alaska (Ebert et al. 2008; Gburski et al. 2007), British Columbia (McFarlane and King 2006), U.S. West Coast (Thompson 2005), and Monterey Bay, California (Zeiner and Wolf 1993) based on counts of growth zones observed in vertebral centra and visual assessment of maturity stage. Consequently, it is still unknown whether the conflicting results between studies indicate regional variability in growth and maturity

or are solely an artifact of differing interpretation of biological structures among studies. King et al. (2017) found considerable differences in age interpretation among regional agencies responsible for Longnose Skate ageing. A validation study was conducted to address the disagreement and corroborated the methodology outlined in Gburksi et al. (2007) (King et al. 2017).

We seek to resolve the observed discrepancies in growth and maturity estimates among published studies. To that end, we explore the scale and magnitude of spatial variation in growth and maturation of Longnose Skates along their geographic range using a single, validated age-estimation protocol. We hypothesize that Longnose Skates will exhibit a latitudinal gradient in size-at-age and maturity with larger size-at-age (Atkinson 1997) and larger size-at-maturity (Heino and Deickmann 2002, Beacham 1987) at higher latitudes.

1.3 METHODS

1.3.1 *Sample Collection Methods*

Age structures and visual maturity assessments were collected from Longnose Skates during three fishery-independent surveys between the years 2011-2018. In 2011, 2012, and 2018, samples were collected off the coasts of Washington, Oregon, and California on the National Marine Fisheries Service (NMFS) West Coast bottom trawl survey between the months of May and October. In 2015, samples were collected in the Gulf of Alaska on the NMFS Gulf of Alaska bottom trawl survey between the months of May and August. In 2018, samples were collected in the eastern Gulf of Alaska and off the coast of British Columbia on the International Pacific Halibut Commission (IPHC) longline survey between the months of June and August.

The procedures for sample collection varied by survey type. For the NMFS West Coast bottom trawl, biologists randomly selected two Longnose Skates per trawl haul in 2011, but only one

Longnose Skate per trawl haul in 2012 and 2018. Total length, sex, and weight were recorded in all years and visual maturity stage was recorded in 2018. Vessels fished between 55 m and 1,280 m, covering the majority of the Longnose Skate's depth range. On the NMFS Gulf of Alaska bottom trawl survey, one Longnose Skate was selected for age specimen extraction and maturity assessment every other haul where only one Longnose Skate was present. Two Longnose Skates were sampled if that haul had two or more Longnose Skates present using a random number table to avoid size bias. In 2015, the survey fished between 15 m and 1,000 m. Total length, sex, weight and maturity stage were also recorded. The IPHC survey fished with longline gear and Longnose Skates were selected opportunistically for age specimen extraction and maturity assessment based on a length-stratified sampling design (length bins <91 cm, 91-120 cm and, 3) >120 cm); up to fifty skates per sex in each length bin were collected. Vessels fished between 17 m and 732 m. Total length, sex and weight were also recorded.

Vertebrae are the most commonly used structure for age determination of Longnose Skates. They were collected at sea by removing a segment of the vertebral column containing at least five vertebrae. Each specimen was weighed and measured for total length (tip of the snout to tip of the tail). Sex was determined by the presence or absence of pelvic claspers. Maturity stage was determined via a visual assessment of reproductive structures according to Matta and Gunderson (2007) for specimens collected on all three surveys. Maturity data were collected on the NMFS West Coast bottom trawl survey for the first time in 2018 and therefore the specimens collected in 2011-12 used for age estimation on the U.S. West Coast are lacking corresponding maturity data.

1.3.2 *Laboratory Methods*

We processed vertebrae for age determination at the Alaska Fisheries Science Center Age and Growth Program laboratory. First, we removed at least three vertebral centra per specimen from

the frozen vertebral column collected at sea, then cleaned off residual tissue and stored them in 95% ethanol. Next, one vertebra per specimen was mounted in a block of resin and a 0.4 mm section was taken sagittally through the focus (Figure 1.1, Figure 1.2). Sections were viewed underwater against a dark background under reflected light using a dissecting microscope. We took images of each section and enhanced in Adobe® Photoshop® to clarify the annual banding pattern (Figure 1.3) (Campana, 2014). Specimens were aged according to the validated age determination protocol outlined in Gburski et al. (2007).

1.3.3 *Statistical Methods*

One analyst estimated ages for all specimens and two additional analysts estimated age for a subset of specimens to evaluate observation error. There are two types of error associated with age estimation studies: process error and observation error. Process error is due to any deviation in the aging structure's banding pattern relative to the fish's true age. Observation error is due to the ambiguous nature of many species' aging structures that results in inaccurate interpretation of the banding pattern. We did not address process error in this study, however King et al. (2017) found evidence using bomb radiocarbon analysis to support annual banding occurring in Longnose Skate vertebrae. To evaluate observation error, two additional, experienced age analysts generated age estimates for 45% of samples. Precision and bias are two common metrics used to quantify observation error (Kimura and Anderl, 2005). To evaluate precision, we calculated the coefficient of variation (CV) (Chang 1982). McBride (2015) found that CV tracks precision better than other commonly used measures, such as average percent agreement (APE). We evaluated bias visually using age bias plots (McBride 2015). Specimens were excluded from further analysis when any

of the three analysts deemed them of insufficient quality to produce reliable age estimates (i.e., patterns were too faint or vague to generate a single age estimate).

We explored spatial variability in the size-at-age of Longnose Skates from the Gulf of Alaska to Southern California at multiple scales. First, we explored regional variability among the three regions: 1) western and central Gulf of Alaska, 2) eastern Gulf of Alaska and British Columbia, and 3) the U.S. West Coast. We defined the boundary between regions 1 and 2 as that used in stock assessments to delineate between central and eastern Gulf of Alaska (longitude 140.00°W), a known biogeographic breakpoint, and that between region 2 and region 3 at latitude 49.00°N, which corresponds to the northern boundary of the U.S. West Coast stock assessment (Figure 1.4) (Gertseva et al. 2019, Ormseth 2018). Second, we explored finer scale variability within the U.S. West Coast, which was possible because this region had a high quantity of data. Here, we delineated four subareas (Figure 1.4). Breakpoints were based on the International North Pacific Fisheries Management Commission areas that are also known to correspond to biogeographic breakpoints (Gertseva et al. 2017). These were at latitudes 43.00°N, 40.50°N, and 36.00°N (Figure 1.4).

To test our hypothesis that Longnose Skates will have a latitudinal cline in size-at-age, we modeled growth using the von Bertalanffy equation which is commonly applied to elasmobranch species (Cailliet et al. 2006, Pardo et al. 2013). We sought to evaluate whether parameters of the model were common or distinct among our defined spatial areas. To that end, we fit multiple models representing all combinations of common versus spatially-specific parameters, first among regions and then among the four U.S. West Coast subareas (Figure 1.4). We fit growth models using maximum likelihood and used Akaike Information Criterion correct for small sample size (AICc) to evaluate which models were best supported by the data.

The base model, whereby all parameters were assumed common among regions was:

$$L_i = (L_\infty - L_\infty - L_0 e^{-kt_i} e^{-Kt_i}) \varepsilon_i \quad (1)$$

where L_i is the estimated total length of fish *i*, L_∞ is the asymptotic length parameterized as *q/K*, *q* is the coefficient of anabolism and *K* is the coefficient of catabolism (commonly referred to as the von Bertalanffy growth coefficient), t_i is the age estimate for specimen *i*, L_0 is the integration constant expressing the theoretical length when age is zero (or hatching size) (Cailliet et al. 2006, von Bertalanffy 1957), and ε_i is a log-normal error, where $\varepsilon_i = \exp(v_i)$, where $v_i \sim N(0, \sigma)$.

The hierarchical model allows for the model parameters to be area-specific. For instance, the fully hierarchical model allows all parameters to vary by area:

$$L_{i,j} = (L_{\infty,j} - L_{\infty,j} - L_{0,j} e^{-K_j t_i}) \varepsilon_i \quad (2)$$

$$L_{\infty,j} = q_j K_j$$

where j denotes region or subarea, and parameters K_j, q_j, and $L_{0,j}$ were assumed to follow a normal distribution, each with an estimated mean and variance. Random effects assumed *q* and *k* were independent (covariance of 0). There is disagreement in the literature regarding sexual dimorphism in growth for Longnose Skates (Gertseva 2007; Gburski et al. 2007), but our sample was well balanced by sex so male and female skates were pooled to increase sample size (Table 1.1). We assumed each sample was independent for analysis, though we included some samples that were captured in the same haul. More than one skate per haul was collected in only 25% of all total hauls. More than two skates were collected in only 1.8% of all hauls. Therefore, there were not enough repeated measures within hauls to model the effect of haul explicitly. We retained all

data to increase sample size. We performed model diagnostics to check the model assumption of homogenous variability across groups and to check for outliers.

To explore variability in size at maturity, we estimated the length at which 50% of the population was expected to be mature among regions and subareas. To this end, we applied generalized linear mixed models to the maturity data collected among regions or subareas (Doll and Lauer 2013). The fixed effects quantified the effects of skate length and sex, which are known to influence size at maturity for Longnose Skates (Ebert et al. 2008, Thompson 2005). We did not include age as a fixed effect because we did not have age-estimates for all samples. Spatial effects of region / subarea were included as a grouping variable that allowed for a random slope and intercept. We used only a single specimen per haul to avoid pseudoreplication, which was possible in this analysis because data quantity was not limiting. The model describing maturity was formulated as:

$$logit\, p = \beta X + \gamma U + \varepsilon i \quad (3)$$

where p is the probability of being mature, X is a design matrix of fixed effects, β is the vector of fixed effects coefficients, U is the design matrix of random effects, and γ is the vector of random effects coefficients. Fixed effects included the intercept, length, and sex, while the random effect allowed for variable intercepts and slopes with region / subarea. All variances were considered homogenous. The likelihood therefore equaled:

$$L\,\beta = \prod p i^{Y i} (1 - p i)^{(1 - Y i)} \quad (4)$$

which is the product over all *i* observations. We fit the model with the *lme4* package in R using maximum likelihood. We retained all covariates to be conservative in estimates of uncertainty. We performed model diagnostics to check the model assumption of homogenous variability across groups and to check for outliers.

To calculate length at 50% maturity, we calculated the inflection point of the logistic function for each sex within each region / subarea based on the estimated parameters β and γ in Eq. 3 (Doll and Lauer 2013). We evaluated the magnitude of spatial variability in maturity by comparing estimates of length at 50% maturity among regions / subareas. To determine length at 50% maturity, we calculated the length at the inflection point of each logistic curve. To compare relative rates of achieving maturity among regions, we quantified steepness of the maturity ogives by calculating the slope of the logistic function at length at 50% maturity for each sex within each region / subarea. We bootstrapped 95% confidence intervals using the boot() function in R that refit the model with different combinations of data (500 times) and recalculated slope and length at 50% maturity to create a distribution of values.

1.4 RESULTS

The length distributions of included samples varied by region (Figure 1.4). The range of lengths in region 1 and region 2 were similar: 45 cm to 144 cm in region 1 and 57 cm to 137 cm in region 2 with the majority of samples over 100 cm. Longnose Skates included in the study from region 3 were smaller in general. The length range was 17 cm to 131 cm, with the majority of samples under 100 cm.

We prepared and aged a total of 965 samples but only 839 were interpretable for use in the growth analysis (Table 1.1). Of these, 392 (45%) were analyzed by two additional analysts at the AFSC to quantify observation error. All 144 samples included from region 1 were analyzed by three analysts as it was the training set, 22 out of the 86 total samples included from region 2, and 226 out of the 650 total samples included from region 3.

Observation error varied among regions, but we determined that overall error was acceptable for growth modeling. The overall precision of the three age readers' estimates ($CV = 15.39\%$)

was comparable to that reported in other age and growth studies of skates (Campana 2001, Davis et al. 2007). The precision of age estimates was highest in region 1 ($CV = 5.47\%$), declined slightly in region 2 ($CV = 7.76\%$) and was lowest in region 3 ($CV = 22.42\%$). Overall, there appeared to be little systematic bias between reader 1 and reader 2 or between reader 1 and reader 3 (Figure 1.5). However, in the latter case, there was some discrepancy between reader 1 and 3 for the oldest three age classes. Due to low overall bias, the primary analyst's (reader 1) age estimates were used for growth modeling.

Data and growth model analysis supported the hypothesis that size-at-age of Longnose Skates varied among the three regions following a latitudinal cline (Figure 1.6, Table 1.2). The von Bertalanffy growth model provided a good fit to the data, as the estimated residual standard deviation suggested a coefficient of variation of roughly 11%. The data best supported a growth model with variable parameter estimates for the coefficient of anabolism (*q)* by region, but shared estimates for the coefficient of catabolism (*K)* and L_0 among regions (Table 1.2). This indicates the rate of energy acquisition might be different among regions. The delta AICc of the second-best-fitting models in each case (for region and subarea) were over 7, indicating little support (Burnham and Anderson 2002). Asymptotic length (L_∞), parameterized as *q/K*, was imprecisely estimated due to small sample size of older/larger samples that did not constrain the model, and the apparent low curvature of the size-at-age relationship. The differences in size-at-age were greatest between region 1 and region 2. An age-14 Longnose Skate from region 1 was on average 12 cm larger than a Longnose Skate of the same age from region 2, which was on average 5 cm larger than a 14-year-old Longnose Skate from region 3 (Table 1.3). Age 14 was selected for comparison due to small sample size of individuals over the age 14 years in the U.S. West Coast.

At a finer scale within region 3, the model selection did not support the hypothesis of spatially-variable growth (Figure 1.7, Table 1.4). This may in part be due to a small sample size at the upper age range in subareas 2-4, which limited power to detect variation in size-at-age. Consequently, the model provided a good fit to the younger (<15 yr) fish but poor fits to older (>15 yr) fish in region 1.

A total of 618 Longnose Skates (267 males and 351 females) were included in the regional analysis of size at maturity ranging in location from the Gulf of Alaska to Southern California (Table 1.1). Immature skates were more common than mature skates – 63% of male skates and 80% of female skates were immature. For most regions except for region 2, there were more than 20 individuals in each sex and maturity category. Region 2 was the only region that had fewer than 20 individuals in any category.

The size at which Longnose Skates matured varied both by sex and among the three regions (Table 1.5, Figure 1.8). Females matured 27.28 cm larger on average than males. Longnose skates matured at larger sizes (>20 cm) in region 1 compared to region 3 (based on length at 50% maturity; Figure 1.8). There was more uncertainty around length at 50% maturity estimates in region 2, likely due to the small sample size of mature individuals that we included in the analysis. The length at 50% maturity estimates indicated that Longnose Skates in region 2 matured at smaller sizes than region 1 and larger sizes than region 3 (region 1 = M: 99 cm, F: 112 cm; region 2 = M: 85 cm, F: 102 cm; region 3 = M: 74 cm, F: 93 cm) (Table 1.5). There was not a strong indication that the rate of maturation (slope of the relationship at the inflection point) varied among regions. There were some differences in the maximum likelihood estimates among regions but these differences were small relative to the bootstrapped confidence intervals. There was a slight indication of lower slope for region 3 relative to region 1 (Figure 1.8).

A total of 380 Longnose Skates (154 males and 226 females) were included in the finer scale exploration of maturity along the U.S. West Coast (region 3) (Table 1.1). More immature than mature skates were collected – 77% of male skates and 88% of female skates included in the analysis were immature. There were three categories that had fewer than 5 samples included in the analysis.

These data supported finer scale variability in size at maturity along the U.S. West Coast, but this finding could be due to small sample sizes of mature individuals (Table 1.1). A likelihood ratio test indicated that the data supported the inclusion of a random effect of subarea. Maximum likelihood point estimates for length at 50% maturity were highest in subarea 1 (Male: 79.78 cm, Female: 95.75) and lowest in subarea 2 (Male: 63.12, Female: 80.04). However, 95% confidence intervals overlapped between the two subareas. There was complete overlap in length at 50% maturity estimates between subareas 3 and 4, and their bootstrapped 95% confidence intervals overlapped with respect to both subarea 1 and subarea 2 (Figure 1.8). There was high uncertainty around estimates of slope at length at 50% maturity in all subareas, and bootstrapped 95% confidence intervals overlapped among all.

1.5 DISCUSSION

The life processes of growth and maturity often vary spatially within fish species (Adams et al. 2018; Carlson and Parsons 1997; Gertseva et al. 2017, Williams et al. 2016). Our analyses show that the size-at-age and length at 50% maturity of Longnose Skates varied at broad spatial scales following a latitudinal gradient, but did not provide strong support for finer scale variability within the U.S. West Coast region. These findings suggest that disagreement among prior life history studies may be, in part, due to spatial variation along the Longnose Skate's range. However, the pattern in variation does not fully align with past studies (Table 1.6, **Error!**

Reference source not found.), suggesting that reported differences are also likely due to methodological inconsistency (Ebert et al. 2008; Gburski et al. 2007: McFarlane and King 2006; Thompson 2006; Zeiner and Wolf 1993). Our findings also provide information that may improve the application of size-based assessment along the range of the species.

Past studies do not uniformly demonstrate a latitudinal cline in size-at-age for Longnose Skates, however our findings suggest that the size-at-age of Longnose Skates does increase with latitude. In prior studies, the largest asymptotic size was estimated in the Gulf of Alaska (Gburski et al. 2007) and the smallest in Monterey Bay off the coast of California (Zeiner and Wolf 1993), with asymptotic size in British Columbia estimated intermediate between the two (McFarlane and King 2006) (Table 1.4). However, Thompson (2005) estimated growth along the U.S. West Coast north and south of Cape Mendocino and found asymptotic length for both to be substantially larger than that previously reported by Zeiner and Wolf (1993) for California (Monterey Bay). Additionally, the comparison of findings from Thompson (2005) to Gburski et al. (2007) and McFarlane and King (2006), would suggest that size-at-age along the U.S. West Coast is comparable to size-at-age further north, which is in contradiction to our present findings. Therefore, while spatial variability in growth may contribute to the inconsistent findings among studies, differences are also likely caused by dissimilarities in age-determination protocol.

We found larger size-at-age across all regions than reported in previously published studies (Table 1.6). There are several explanations for this. First, our age-estimation criteria likely differed from that utilized in past studies (King et al. 2017). In this study, we applied the validated age estimation methodology outlined in Gburksi et al. (2007), and our von Bertalanffy parameter estimates most closely align with that study. The difference we observe in asymptotic size between these two studies could be due to differences in modeling approaches. Second, we

utilized a hierarchical modeling approach which allowed us to "share" information between regions with larger sample sizes (Adams et al. 2018). We found this approach to be more biologically realistic as it accounts for the fact that Longnose Skates in different regions are still the same species with parameter estimates that will be related to one another. Third, asymptotic length was not well constrained due to a low sample size of larger bodied and older individuals. Therefore, maximum likelihood estimates were strongly influenced by the high quantity of younger/smaller samples and did not fit the relatively less common larger samples particularly well. This seems to be a consistent issue across studies. This may suggest that larger bodied Longnose Skates are relatively rare, or that current sampling techniques are not able to access them. Longnose Skates do not seem to reach asymptotic length within the range of ages commonly sampled, and may rarely do so within their life span. Therefore, L_{∞} is estimated imprecisely and we instead compared length-at-age between regions based on predicted length at a common age (14 years).

Our findings supported a latitudinal gradient in length at 50% maturity with individuals maturing at larger sizes in region 1 and smaller sizes in region 2 and region 3 (Table 1.5, Figure 1.8). Despite differences in length at 50% maturity among the three regions of our study area, calculations for age at 50% maturity (from our von Bertalanffy growth model) were similar among regions (Male = 8-10 years, Females = 9-13 years). This suggests that maturity may be driven by age for Longnose Skates but because we estimated age at 50% maturity outside of the model, this hypothesis requires more exploration. Our data may support finer scale variability in maturity along the U.S. West Coast. Point estimates differ slightly among subareas, particularly for the subarea along the coast between Cape Blanco and the Columbia River; however, the small sample size of mature individuals increased uncertainty and rendered large differences

unlikely (Table 1.1, Figure 1.8). More conclusive results may be achieved by increasing the sample size, especially of mature individuals.

Inconsistencies in length at 50% maturity estimates among studies are likely due to inconsistency in maturity determination criteria (**Error! Reference source not found.**). Our estimates of length at 50% maturity in region 1 are within several cm of those estimated by Ebert et al. (2008) for the Gulf of Alaska, which lends confidence to our findings. Results in Ebert et al. (2008) were attained using histology, which is generally regarded as the most robust approach for assessing reproductive stage (Vitale et al. 2006). McFarlane and King (2006) estimated notably smaller length at 50% maturity for samples from British Columbia than region 2 of the present study. However, this is likely because McFarlane and King (2006) used different criteria for their maturity staging, classifying skates as mature that all other studies classified as adolescent or maturing. Our estimates for length at 50% maturity in region 3 along the U.S. West Coast are similar to those reported for samples south of Cape Mendocino in Thompson (2005). However, Thompson (2005) estimated larger length at 50% maturity along the U.S. West Coast north of Cape Mendocino than we report in any of the 3 regions. One possible explanation suggested by Thompson (2005) is that her estimates of length at maturity might have been overly high due to a conservative methodology used for maturity staging. It is unclear why that would have disproportionately affected length at 50% maturity estimates north of Cape Mendocino relative to the south but could be due to bias introduced from length distribution of the sample.

The observed spatial variability in length and maturity suggests that the current management scale is likely sufficient to capture life history variability for this species along the U.S. West Coast. Currently, Longnose Skates are assessed in three separate assessments: the U.S. West Coast, British Columbia, and the Gulf of Alaska. Along the U.S. West Coast, Longnose Skates

are managed as one continuous stock (Gertseva et al. 2019). We did not find strong evidence for finer scale variability in growth and maturity along the U.S. West Coast, which supports applying the same growth and maturity parameters to the entire region. Since our sample sizes in the maturity analysis were small, more robust results could be attained by redoing this analysis with more samples. Within the Gulf of Alaska, the region is further divided into western, central, and eastern, each assigned with separate harvest recommendations (Ormseth 2018). Our findings support differences in size-at-age and size-at-maturity between the western and central Gulf of Alaska management areas relative to the eastern Gulf of Alaska management area. This suggests that a finer scale exploration of growth and maturity within the Gulf of Alaska assessment area may be warranted. In British Columbia, the stock is further divided into four separate management areas (King et al. 2015). We did not have high enough representation of samples from the British Columbia assessment area to model finer scale variability within this region, but increasing sample size in the future would allow for finer scale variability to be explored.

Variability in the growth and maturity of Longnose Skates has long been suspected based on conflicting results in the published literature (Ebert et al. 2008; Gburski et al. 2007; McFarlane and King 2006; Thompson 2006; Zeiner and Wolf 1993). By using a validated age reading protocol and standardizing age estimation and maturity assessment criteria across their geographic range, the results of this study suggest that there is spatial variability from the Gulf of Alaska to Southern California in the growth and maturity of Longnose Skates. The extent to which life history information on growth and maturity is currently incorporated into assessment varies. However, we provide information that can improve the future application of size-based assessment along the range of the species. Incorporating robust life history information into stock

assessments may allow us to make more informed management decisions with the goal of maximizing economic yield while ensuring sustainability of this elasmobranch species.

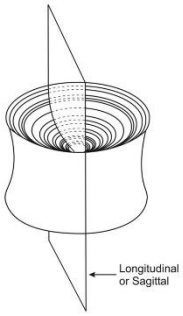

Figure 1.1. Illustration of elasmobranch vertebral centrum and sectioning plane used for age determination. Adapted by Wendy Carlson (AFSC Graphics Unit) from G.M. Caillet and K. J. Goldman.

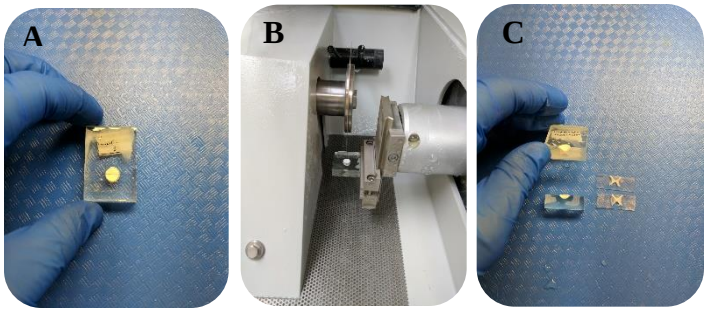

Figure 1.2. A) Longnose Skate vertebra in resin. B) Block mounted in saw ready for sectioning. C) Two 4 mm sections cut sagitally through the focus of the vertebra ready for age-determination.

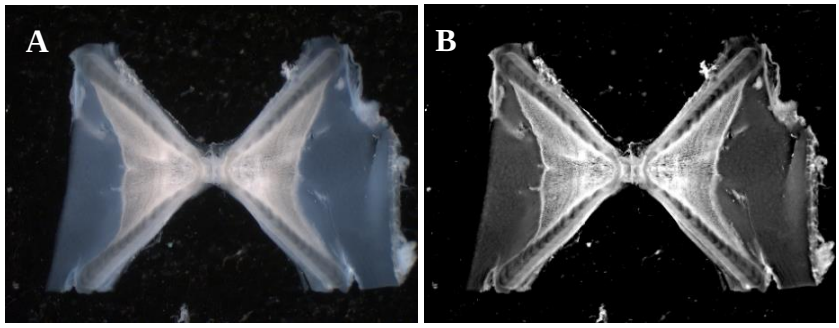

Figure 1.3. A) Longnose skate vertebra (estimated age = 12 year) before image enhancements. B) Same vertebra after enhancements in Adobe Photoshop.

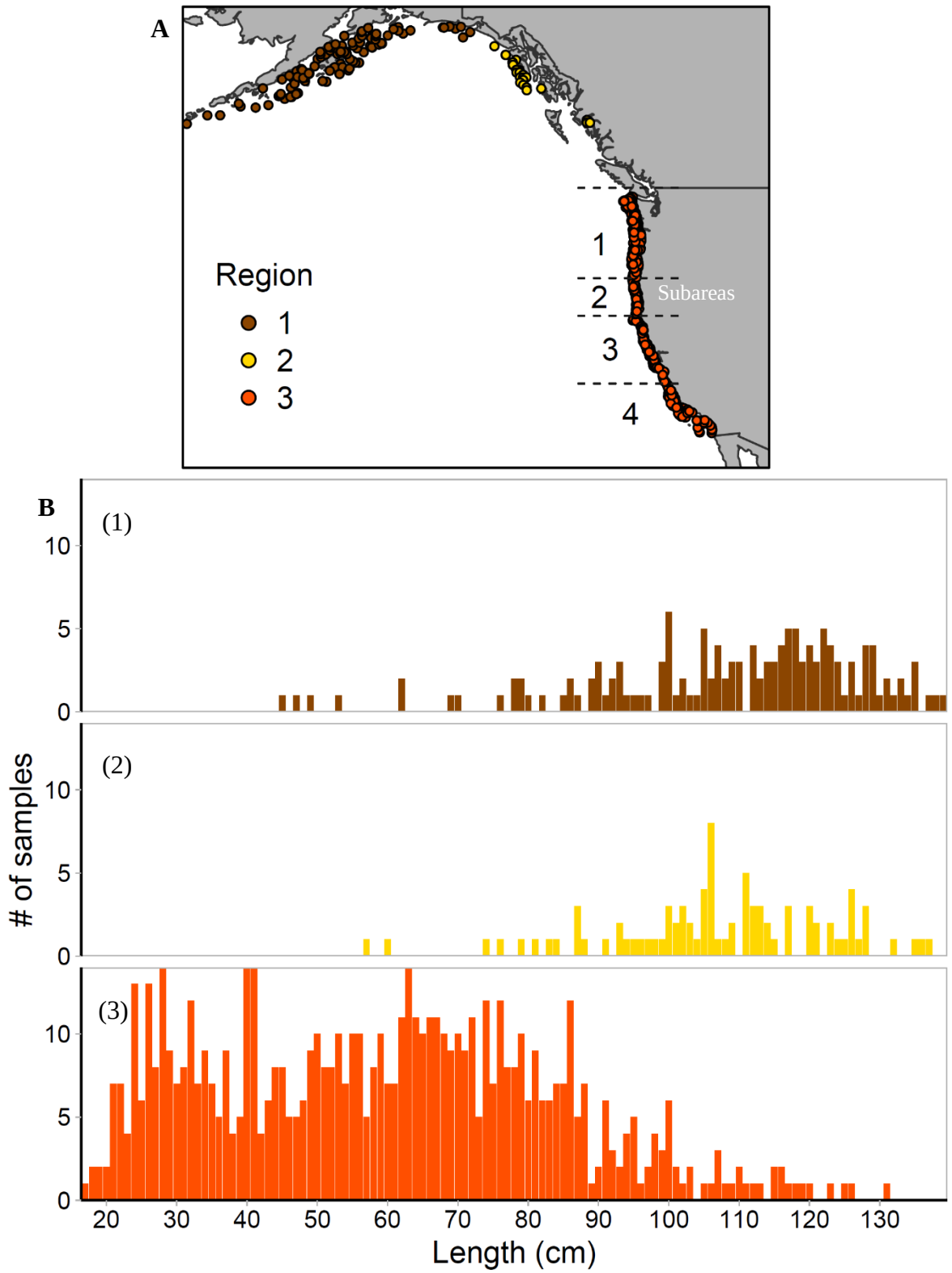

Figure 1.4. A) Longnose Skate catch locations for the three regions: western and central Gulf of Alaska (1), eastern Gulf of Alaska and British Columbia (2) and U.S. West Coast (3). B) Length distributions of specimens used in growth and/or maturity analysis in the three regions.

Table 1.1 Sample sizes for length-at-age analysis and maturity analysis by a) region and b) subarea.

a.

		Maturity data sample size			
		Male		Female	
Region	**Age data sample size**	Immature	Mature	Immature	Mature
1	141	31	41	62	26
2	86	18	24	21	16
3	650	119	34	199	27
Total	**839**	**168**	**99**	**282**	**69**

b.

		Maturity data sample size			
		Male		Female	
Subarea	**Age data sample size**	Immature	Mature	Immature	Mature
1	284	53	15	104	15
2	82	13	7	16	5
3	138	29	6	37	4
4	146	24	6	42	3
Total	**650**	**119**	**35**	**199**	**27**

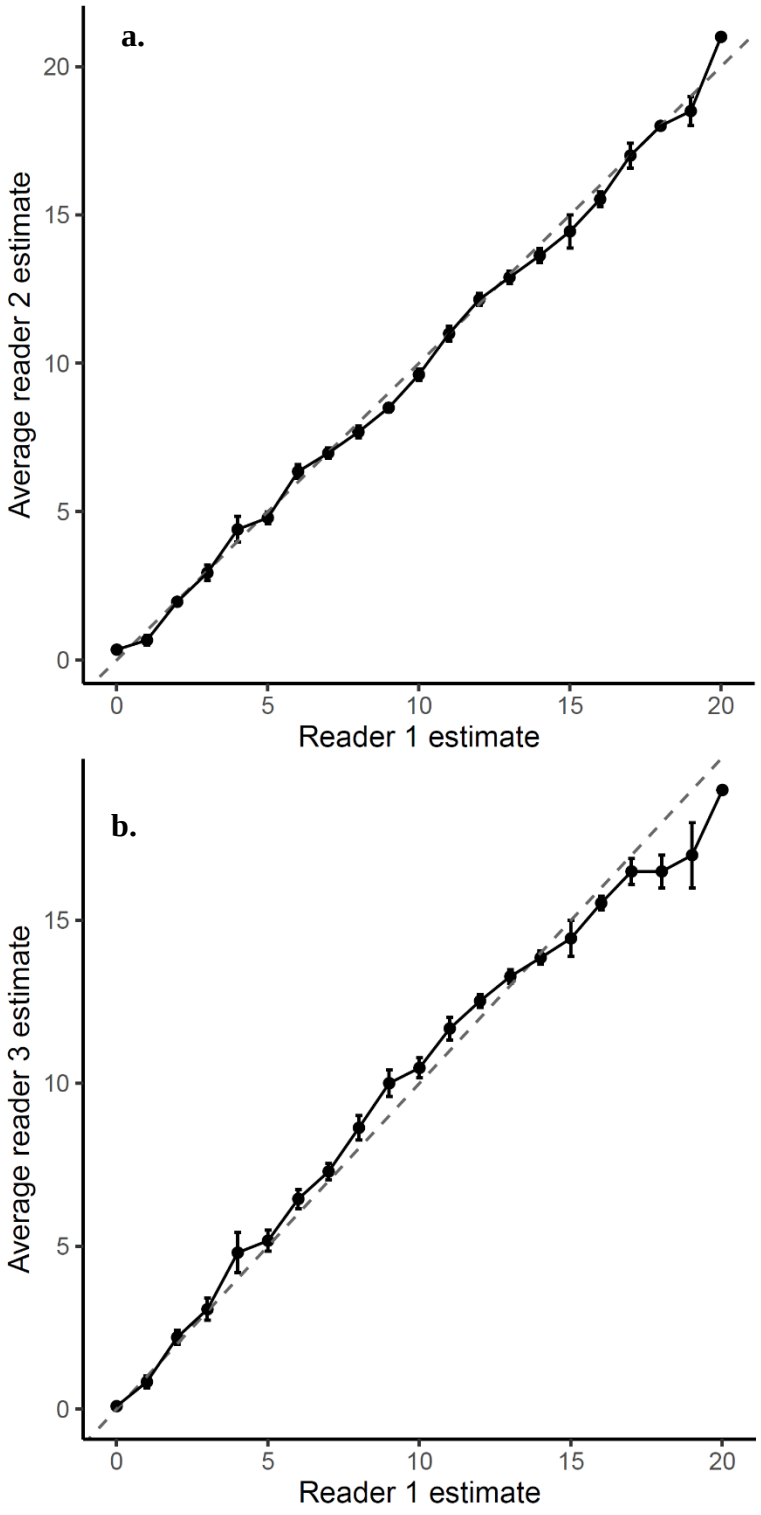

Figure 1.5. a) Average reader 2 and b) average reader 3 age estimates compared to reader 1 estimates with error bars showing +/- standard error. Dashed line represents 1:1 agreement.

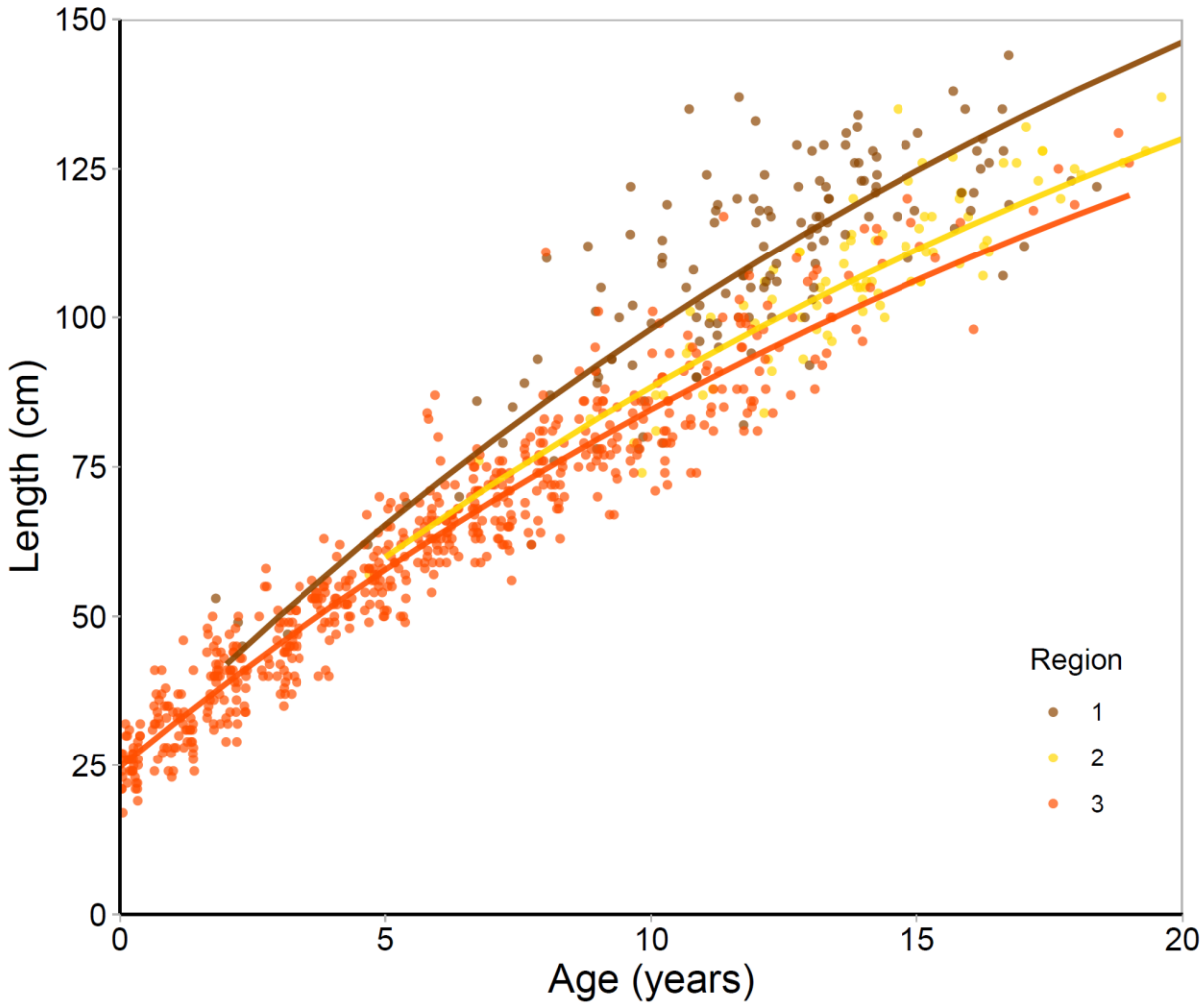

Figure 1.6. Best fitting von Bertalanffy growth functions fit to length-at-age data for region 1 (brown), region 2 (yellow), and region 3 (orange).

Table 1.2. AICc scores for hierarchical von Bertalanffy growth models allowing for regional variability in parameter estimates. The data best supported a model with regional variability in *q*, the coefficient of anabolism.

Model	AICc	ΔAICc	# Parameters
Fixed *K*, L_0, regional *q*	-1379.68	0	8
Fixed *q*, *K*, regional L_0	-1371.69	7.99	8
Fixed L_0, regional *q*,*K*	-1371.48	8.20	12
Fixed *q*, L_0, regional *K*	-1365.49	14.19	8
Fixed *K*, regional *q*, L_0	-1365.15	14.53	12
Fixed *q*, regional *K*, L_0	-1363.55	16.13	12
Regional *q*, *K*, L_0	-1354.88	24.80	16
Fixed *q*, *K*, L_0	-1217.95	161.73	4

Table 1.3. Von Bertalanffy parameter estimates fit via maximum likelihood. Numbers in brackets are standard error. Length at age 14 (L_{14}) was calculated after fitting the von Bertalanffy function and standard error for the estimates was calculated using the delta method. Parameter estimates for $\bar{q}$, σ_q, *K*, L_0, and σ were shared among all regions and were in order: 9.09 [0.53] year^{-1}, 0.71 [0.29], 0.04 [0.005] year^{-1}, 24.75 [0.27] cm, and 0.11 [0.003].

Region	L_{14} (cm)	q year^{-1}
1	119.81 [0.59]	10.04 [0.38]
2	107.90 [0.72]	8.84 [0.38]
3	102.28 [2.67]	8.38 [0.27]

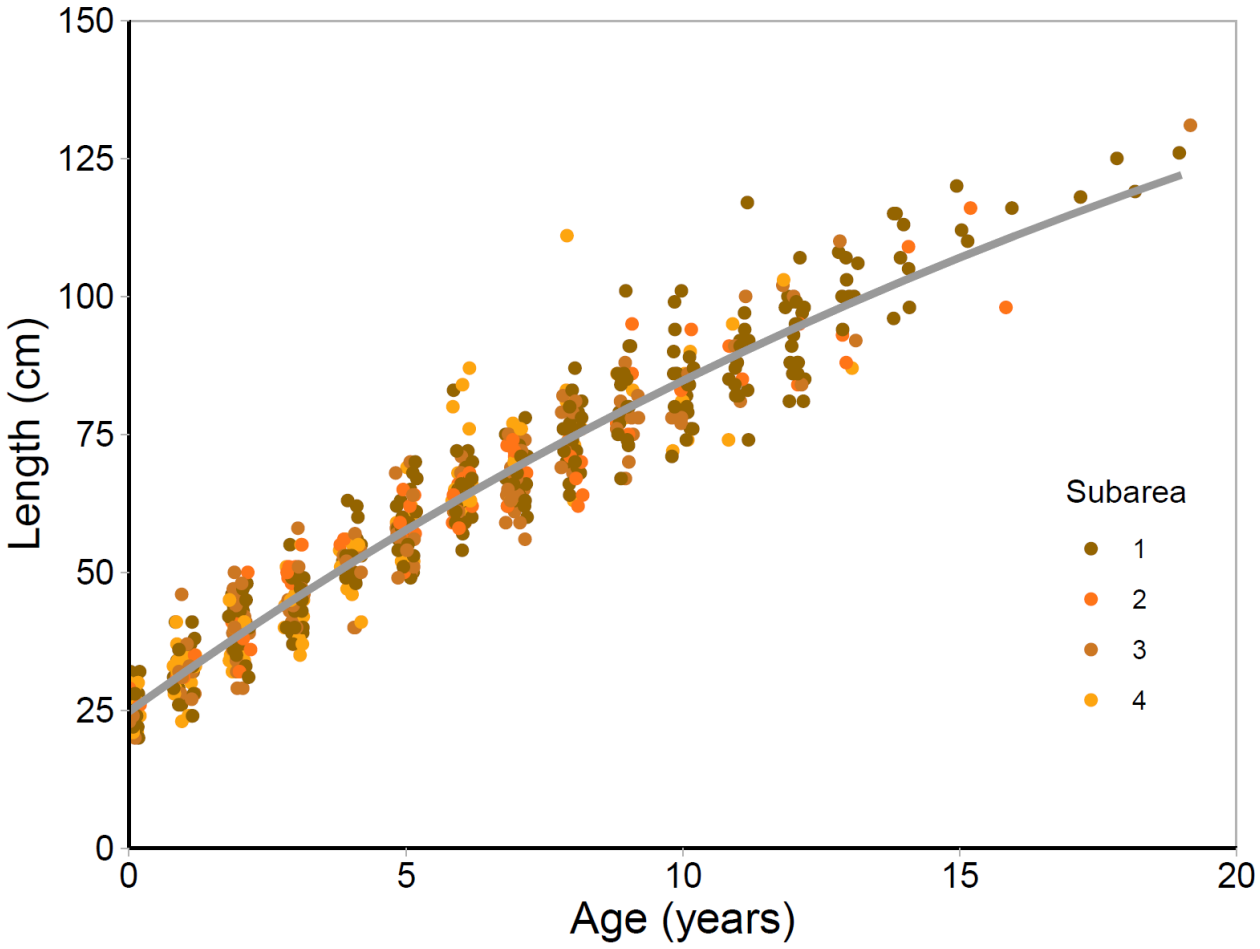

Figure 1.7. Three parameter von Bertalanffy growth function fit to length-at-age data for the U.S. West Coast.

Table 1.4. AICc scores for hierarchical von Bertalanffy growth models allowing for subarea variability in parameter estimates. The data do not reveal any variability between subareas.

Model	AICc	ΔAICc	# Parameters
Fixed *K*, L_0, *q*	-1007.60	0	4
Fixed *q*, *K*, subarea L_0	-998.35	9.31	9
Fixed L_0, *K*, subarea *q*	-997.38	10.22	9
Fixed *q*, L_0, subarea *K*	-997.38	10.22	9
Fixed *q*, subarea *K*, L_0	-987.97	19.69	14
Fixed L_0, subarea *q*, *K*	-986.99	19.69	14
Subarea *q*, *K*, L_0	-977.41	20.61	14
Fixed *K*, subarea *q*, L_0	-896.26	30.25	19

Location	**Sex**	**N**	**L50 (cm)**	**Slope at L50**
Western and Central Gulf of Alaska	M	72	99.12 [94.71, 103.35]	0.04 [0.02, 0.05]
	F	88	111.81 [108.32, 115.37]	0.04 [0.02, 0.05]
E. Gulf of Alaska and British Columbia	M	72	84.85 [76.33, 95.41]	0.03 [0.01, 0.04]
	F	88	102.34 [92.56, 109.74]	0.03 [0.01, 0.04]
U.S. West Coast	M	153	73.83 [69.49, 79.02]	0.02 [0.02, 0.03]
	F	226	92.52 [87.48, 98.75]	0.02 [0.02, 0.03]

Table 1.5. Length at 50% maturity (L50) estimates and slopes of maturity ogives at L50 for each region. Numbers in brackets are standard error.

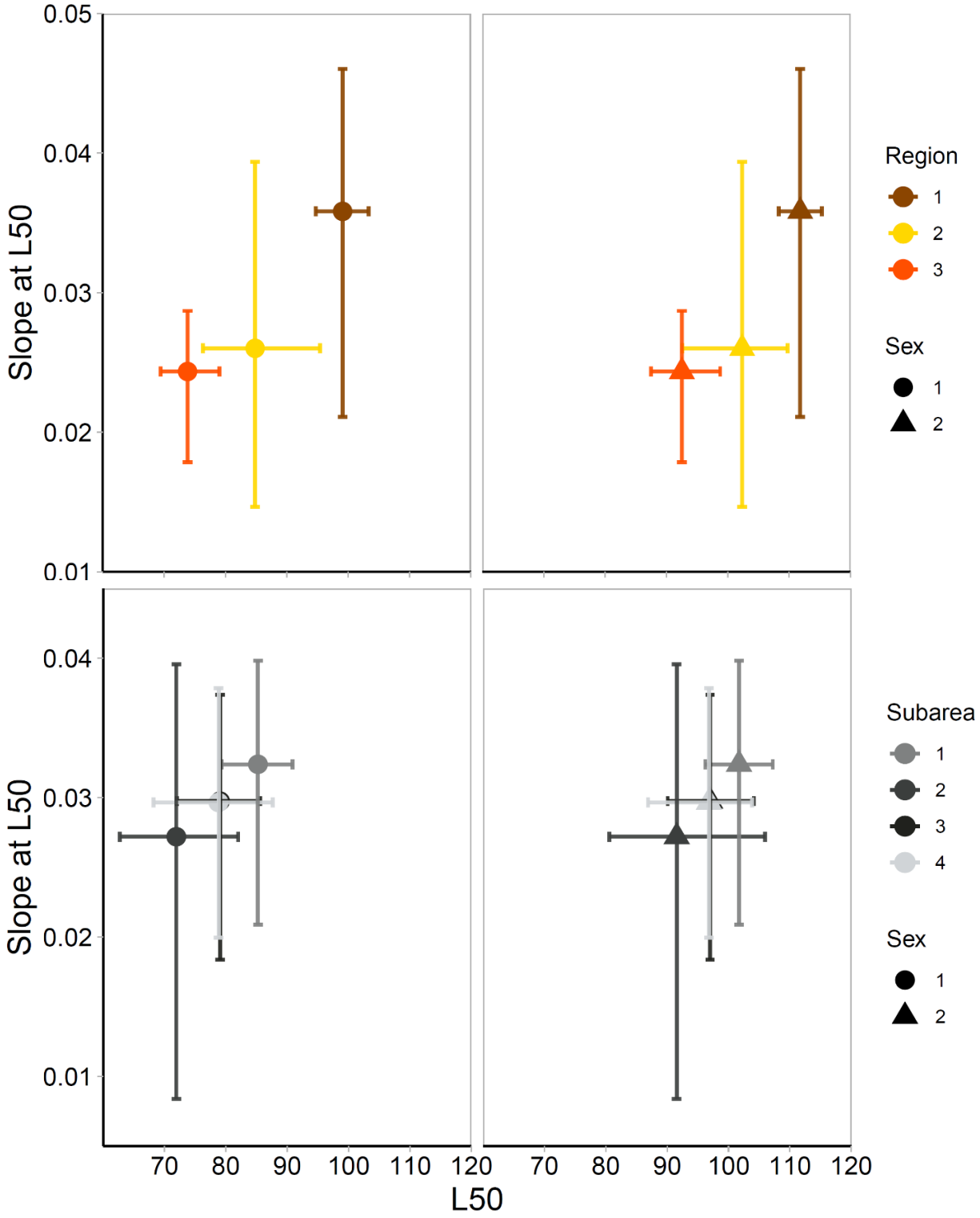

Figure 1.8. Length at 50% maturity estimates with bootstrapped 95% confidence intervals for males (left) and females (right) in three regions (top) and four subareas along the U.S. West Coast (bottom).

Table 1.6. Comparison of estimated von Bertalanffy growth parameters and maximum ages found for Longnose Skates in five different studies. Only point estimates reported. *C designates combined estimate for both sexes.

Location	**Source**	**Sex**	**N**	**Max Age (yrs)**	**L_∞ (cm)**	**k**
Gulf of Alaska	Gburski et al. 2007	M	48	25	C: 203.8	C: 0.04
		F	55	24		
Western and Central Gulf of Alaska	This study	M	65	20	C: 251	C: 0.04
		F	76	18		
British Columbia	McFarlane and King 2006	M	117	25	131.5	0.07
		F	125	26	137.2	0.06
Eastern Gulf of Alaska/ British Columbia	This study	M	46	19	C: 221	C: 0.04
		F	39	20		
U.S. West Coast (North)	Thompson 2005	M	79	22	C: 170.0	0.06
		F	82	20		
U.S. West Coast (South)	Thompson 2005	M	67	16	C: 138.3	0.07
		F	86	15		
Monterey Bay	Zeiner and Wolf 1993	M	64	13	95.2	0.16
		F	68	12	106.9	0.26
U.S. West Coast	This study	M	317	16	C: 209.5	C: 0.04
		F	328	19		

Error! Reference source not found. Comparison of estimated of length and age at 50% maturity and maximum length found for Longnose Skates in five different studies. Only point estimates reported.

Location	Source	Sex	N	Max Length (cm)	L 50 (cm)	A50 (yrs)
Gulf of Alaska	Ebert et al. 2008	M	354	136	102.9	--
		F	318	142	113.1	
Western and Central Gulf of Alaska	This study	M	72	133	99.11	10
		F	88	144	111.81	12-13
British Columbia	McFarlane and King 2005	M	117	122	65.0	10
		F	125	125	83.0	13
Eastern Gulf of Alaska/ British Columbia	This study	M	42	135	84.85	9
		F	37	137	102.34	13
U.S. West Coast (N)	Thompson 2005	M	82	130	108.0	14
		F	82	135	120.0	16
U.S. West Coast (S)	Thompson 2005	M	67	102	81.0	11
		F	86	100	90.0	13
Monterey Bay	Zeiner and Wolf 1993	M	64	132	--	--
		F	68	107		
U.S. West Coast	This study	M	153	117	73.83	8
		F	226	131	92.52	12

Chapter 2. RAPID AGE ESTIMATION OF LONGNOSE SKATE (*RAJA RHINA*) VERTEBRAE USING NEAR INFRARED SPECTROSCOPY

2.1 ABSTRACT

Accurate age data are an important component of assessing and managing fish populations, yet traditional age estimation methods for elasmobranchs are time consuming, expensive, and imprecise. The use of near infrared spectroscopy is a novel approach to age estimation that has shown promising results for use on several species of sharks. We explored the use of Fourier transform near infrared spectroscopy (FT-NIRS) to predict age for a batoid species, the Longnose Skate (*Raja rhina).* The Longnose Skate is one of a small number of elasmobranch species for which annual band periodicity has been validated, allowing for traditional age estimation and making it an ideal candidate for this study. To evaluate the error associated with existing age estimation methods, we first compared the precision and bias of traditional age estimates among agencies responsible for aging Longnose Skates. This provided a baseline for comparison to evaluate the error associated with the FT-NIRS technology. We then explored the use of FT-NIRS to derive age estimates from vertebral centra of a batoid species. We used age estimates from the primary reader (reader 1) generated based on validated age estimation protocol to build a predictive model between near infrared spectra and skate age estimates. The model fit the data well, with r-squared value of 0.81 (RMSE = 1.91 years). When externally validated with a separate data set, the model had an r-squared of 0.87 and a RMSE of 1.45 years, indicating model predictions were within 1.45 years of the traditionally generated age estimate 68% of the time. Precision between FT-NIRS predictions and reader 1 age estimates (CV = 29.46%) was lower than precision between readers using traditional methods (CV = 12.93%). Bias was reduced through the mid age range (3-

15 years) relative to traditional methods, but still present at the lower and upper age ranges. The results of this study suggest that it is possible to calibrate a model with a good ability to predict Longnose Skates ages from the near infrared spectra of their centra more efficiently than via traditional methods. However, improved efficiency is paired with a reduction in precision and a shift in bias structure. This is important because while these methods allow for more regular acquisition of a higher quantity of age data, it will be important to account for an associated difference in aging error if this data type is incorporated into stock assessments.

2.2 INTRODUCTION

Information on the age of fishes is an essential component of fisheries research and management. Accurate age data allow for a more robust understanding of population dynamics and improve our ability to conserve and manage species effectively. Fish age is used in aged-structured assessment methods and used to estimate growth rate, mortality rate, age at maturity, and longevity. Imprecise or inaccurate age estimates can preclude effective conservation and management (Campana 2001, Lai and Gunderson 1987). Barnett et al. (2013) found that age at maturity relative to total lifespan impacted estimates of population growth rate for five deep water skates in the Bering Sea. This illustrates the importance of both having information on fish age, but also ensuring that that information is accurate. Otherwise, our understanding of population dynamics and resulting conservation and management decisions may be ineffective (Campana 2001).

Maintaining contemporary age data is also important to ensure accurate understanding of population dynamics because size-at-age can fluctuate over time (Stawitz 2017). Growth can be altered by factors such as ecological and environmental conditions (Shelton and Mangel 2012), fishing mortality (Heino and Dieckmann 2008), and density dependent effects (Lorenzen and Enberg 2001). Environmental conditions such as changes in temperature have been shown to effect

fish growth (Matta et al. 2010, Matta et al. 2018, Pistevos et al. 2015). Mortality caused by predation or fishing can impact growth through several mechanisms. Increased mortality can reduce population density leading to increased food availability and faster growth (Heino and Diechmann 2008). Mortality that is size selective toward older and large individuals can favor genotypes that grow faster (Stokes and Law 2000). Tracking changes in growth can lend insight into demographic changes in a population, and doing so is important to maintain accurate parameter estimates used in age-structured assessment methods.

However, many elasmobranchs do not have any age information because they are usually not high valued, targeted species in fisheries, and they lack structures commonly used to age teleost fish (Dulvy et al. 2014; Cailliet 2006; Matta et al. 2017). Though many species are exploited either directly or indirectly, historically there has not been a large research focus on elasmobranch species because they have not supported as many economically valuable fisheries as teleost fishes (Cavanagh et al. 2005). Additionally, acquiring information on their age is especially difficult because elasmobranchs do not possess otoliths, which are commonly used for age-estimation for teleost fishes. Instead, thin sections of their vertebrae are often used for ageing, but this method is time consuming and has not been validated for many species (Matta et al. 2017). Validation is important to ensure that age-estimation protocol yields biologically accurate age estimates.

The Longnose Skate is one of the few species of elasmobranch for which age estimation methods are validated (King et al. 2017). However, traditional age estimation from thin sections of vertebrae is expensive and time consuming, which precludes routine age estimation. Fourier transform near infrared spectroscopy (FT-NIRS) is an emerging technology in the field of fish aging used to more efficiently estimate teleost ages from otoliths and shark ages from vertebrae (Helser et al. 2018,

Rigby et al. 2016, Wedding et al. 2014). Using FT-NIR, it may be possible to increase the quantity and frequency of age estimation for elasmobranch species without sacrificing accuracy.

Fourier transform near infrared spectroscopy is a technique that uses light in the near infrared spectrum to determine the chemical composition of a material. Chemical compounds absorb light at different frequencies based on their unique molecular structures. A FT-NIR spectrometer measures absorbance of a material across a range of wavelengths and produces a unique spectrum per sample. Chemometric techniques are then used to analyze the spectrum to deduce chemical composition (Robins et al. 2015). This includes building a calibration model between a "known" substance and its near infrared spectrum. Near infrared spectroscopy is used routinely in many other industries such as agriculture and pharmaceuticals to measure chemical constituents (McClure et al. 2002, Roggo et al. 2008). In the case of fish aging, the known substance is a known or estimated age. Therefore, the ability to predict fish age using FT-NIRS is founded on the concept that there is a relationship between an aging structure's chemical composition and the specimen's age. Because aging methodology is validated for Longnose Skates, we were presented a unique opportunity to evaluate the use of FT-NIRS to estimate ages from the vertebral centra of a batoid species. The objective of this study is to determine whether the use of FT-NIRS could more rapidly generate age estimates for Longnose Skates that are comparable to human age reader estimates.

2.3 METHODS

2.3.1 *Observation error in traditional methods*

Longnose Skate samples were collected during the Gulf of Alaska National Marine Fisheries Service bottom trawl survey from May 29 to August 9, 2015. Vertebrae were collected at sea by removing a segment of the vertebral column and stored frozen preservation. We prepared thin sections for visual age-estimation following protocol in Chapter 1 (this thesis).

Age was estimated for each specimen by three age readers from the Alaska Fisheries Science Center (AFSC). Additionally, we prepared a Longnose Skate age reading manual that illustrates how to interpret growth patterns on Longnose Skate vertebrae based on the validated protocol outlined by Gburski et al. (2007). We initiated an aging structure exchange among the three agencies responsible for estimating ages for Longnose Skates to establish a baseline observation error rate for comparison with FT-NIRS technology. We distributed a set of 30 vertebrae and the Longnose Skate age reading manual to the other two agencies that participate in aging Longnose Skates along the North American west coast: Department of Fisheries and Oceans Canada and the Northwest Fisheries Science Center. This is a sample size within the standard range for an age reading exchange to evaluate the extent of agreement among agencies (Committee for Age Reading Experts, http://care.psmfc.org). Each agency had two age readers estimate ages for the same 30 vertebrae after reading the manual.

There are two types of error associated with age and growth studies: process error and observation error. Process error occurs when growth zones in the aging structure do not reflect true age. Observation error is any error made in human interpretation of the structure. We did not address process error in this study; however, the results of King et al. (2017) suggest annual band periodicity in the vertebrae of Longnose Skates. Observation error was evaluated based on precision (% CV) and bias among age estimates according to methodology outlined in Chapter 1 (this thesis).

2.3.2 *Fourier transform near infrared spectroscopy*

Longnose Skate vertebral centra used for spectroscopic evaluation by the FT-NIRS were provided from a separate study on regional variability in the age and growth of Longnose Skates (Chapter 1, this thesis). There was a small sample size in the Gulf of Alaska used in the inter-agency age

reading exchange, however the large quantity of samples available from the U.S. West Coast from the previous study that had age data associated provided a unique opportunity to evaluate the use of FT-NIRS to more rapidly estimate age of a batoid species.

Samples from Longnose Skates were collected on a National Marine Fisheries Service bottom trawl survey in 2011-2012 between the months of May and October. Vertebrae were collected at sea and stored frozen. Individual vertebrae were then dissected out of the frozen vertebral column and stored in ethanol for preservation. One vertebra per specimen was used for age estimation in the age and growth study (Chapter 1, this thesis) and one for spectroscopic evaluation in this present study. Ages were estimated by counting annually deposited growth bands on vertebral thin sections according to validated protocol (Gburski et al. 2007). We refer to these age estimates as "traditional age" in this present study while "predicted age" is used to represent the age estimated by the FT-NIRS calibration model.

All vertebrae used for spectroscopic evaluation were stored in ethanol following dissection for a variable amount of time but never longer than one week to standardize for potential degradation. We placed one whole vertebra per specimen under a fume hood and allowed it to air-dry for 48 hours. We then placed each specimen on the sampling window of a Bruker TANGO-R Fourier transform near infrared spectrometer in a standardized sagittal orientation and covered with a reflector cap. Absorbance data were acquired at 16 cm^{-1} resolution with 64 co-added scans. We collected spectral absorbance data from 648 vertebrae.

We conducted data analysis in OPUS (version 7.8, Bruker Optics), a chemometric software package. Raw spectral absorbance data, or spectral data, often need to be mathematically transformed to enhance variation between specimens and remove unwanted noise (Robins et al. 2015). We pre-processed raw spectral data using mean centering, quotient normalization, and a 1^{st}

derivative (17-point Savitsky-Golay smooth) transformation. Next, we fit a Partial Least Squares (PLS) regression model between age estimates and the transformed spectral data. PLS is a multivariate regression method commonly used for chemometric analysis (Chen and Wang, 2002; Helser et al. 2018; Rigby et al. 2016). The spectral data collected along the full wavenumber range between 11,500 and 4,000 cm^{-1} contain an abundance of information about the chemistry of the vertebra, not all of which is relevant for estimating age. We used an optimization routine in the software to identify the least amount of spectral data necessary to differentiate among specimens based on age. We selected a random 50% of specimens that encompassed the full range of spectral variation. This subsample was used to calibrate the model between Longnose Skate traditional age estimated by the primary reader and spectral data using leave-one-out cross validation to maximize the model's predictive ability. In this process, each sample is systematically left out and a PLS model is fit to the remaining samples. The parameter estimates are then used to estimate the age of the left-out sample and the mean error of all predictions versus reference ages can be calculated as the root mean square error of cross validation, or RMSE(CV). The remaining 324 specimens were used to externally cross-validate the model and a root mean square error of prediction, or RMSE(P), was calculated as a measure of its predictive ability. Lastly, to assess how FT-NIRS age estimates compared to traditional methods, we assessed precision and relative bias between predicted age and traditional age and compared it to that of traditional methods.

2.4 RESULTS

2.4.1 *Observation error in traditional methods*

The precision of current, traditional methods had a coefficient of variation (CV) of 12.9% among all readers at the three agencies responsible for Longnose Skate age estimation (Figure 2.1). There was a range of different bias structures between reader 1 and readers 2-7 (Figure 2.2). These ranged

from the slight tendency for other readers to overestimate age relative to reader 1 (Reader 3), to substantial underestimation relative to reader 1 (Reader 4 & 5). However, in general, bias was more pronounced at the ends of the age range and less prevalent in the mid-age range (9-14 years).

2.4.2 *Fourier transform near infrared spectroscopy*

Two wavenumber ranges were identified to be the most informative for estimating Longnose Skate age from the spectral absorbance of vertebrae: 5448 – 6104 cm^{-1} and 7496 – 9400 cm^{-1}. These ranges are similar to those identified for otoliths but slightly narrower (Helser et al. 2018). It is unknown which chemical compounds relate to these regions in skate vertebrae.

A calibration model was fit to establish a relationship between light absorbance in these two wavenumber ranges and Longnose Skate age (n=324). Cross-validation yielded a RMSE(CV) of 1.91 years and a coefficient of determination (R^2) of 0.81 (Figure 2.3a). The RMSE(CV) indicates that 68% of the predicted ages from cross-validation fall within 1.91 years of the reference age. The R^2 indicates that over 81% of variation in predicted age is explained by the linear PLS model. When the calibration model was used to predict ages for the remaining 324 samples, it yielded a RMSE(P) of 1.45 years and an R^2 of 0.87 (Figure 2.3b).

Lastly, the precision between FT-NIRS ages estimates relative to reader 1 was compared to the precision among human age reader estimates. The CV of reader 1 estimates relative to the FT-NIRS predictions was 29.46%. Complete agreement between human age readers was 36.6%, compared to 28.4% for FT-NIRS predictions relative to reader 1 (Figure 2.4). However, agreement within 1 year was comparable between the two methods, with 73.8% between reader 1 and readers 2-7, and 75.6% between reader 1 and FT-NIRS predictions (Figure 2.4). We observed a bias in FT-NIRS predictions, with a tendency to over-estimate younger ages (< 2 years) and under-estimate older ages (>14 years) relative to reader 1 (Figure 2.5). Overall, there appeared to be less

bias in FT-NIRS predictions relative to traditional estimates than among age readers along the mid age range (3-14 years) (Figure 2.2).

2.5 DISCUSSION

We explored the use of FT-NIRS to more efficiently estimate the age of a batoid species, the Longnose Skate, from their vertebral centra. Traditional methods of elasmobranch age determination are time consuming, imprecise, and can be biased between readers. The results of this study are comparable to those published for other elasmobranch species and suggest that models can be built with good predictive ability between age and the near infrared spectra of Longnose Skate centra (Rigby et al. 2016). Additionally, while precision of estimates is reduced, there may be an overall improvement with respect to bias, at least in the mid-range ages. This technology has potential to improve the frequency, quantity, and reproducibility of Longnose Skate age data for use in stock assessments and management.

While age estimates generated from the FT-NIRS approach were less precise than age estimates among age readers, our results suggest improvements with respect to bias and reproducibility. Precision among age readers was similar compared to that reported for other elasmobranch species, which frequently do not have CVs under 10% (Campana 2001). However, variable bias was observed between reader 1 and readers 2-7 (Figure 2.2). This illustrates the observation error that exists in traditional age-estimation studies. Human interpretation of aging structures is subject to error which, when unaccounted for, can impact the efficacy of species management (Campana 2001). FT-NIRS can make age predictions more standardized and reproducible among agencies by removing that source of error. The FT-NIRS estimates relative to reader 1 were less precise (CV = 29.46%); however, there was a marked reduction in inter-method bias throughout the mid-age range relative to among age readers (Figure 2.2, Figure 2.5). While bias was still observed in

FT-NIRS estimates, with a tendency to over-estimate age for very young skates and under-estimate age for older skates, the approach is standardized and reproducible, which is an improvement relative to traditional methods. The bias we observed between reader and FT-NIRS estimates may be due to two reasons. First, the calibration model did not contain many old skates, which could affect its predicative capability in that age range. Second, there is a level of observation error associated with the age estimates used to calibrate the model that was not accounted for, as true age of these specimens was unknown. Future work could include using a more balanced dataset to fit the calibration model between spectra and age estimates, as well as utilizing known-age specimens, which may help to resolve this bias.

The results of this study show promise for the use of FT-NIRS to more rapidly and efficiently estimate ages for Longnose Skates. This is important because it may allow for a larger quantity and higher frequency of age estimates to be generated for use in stock assessment. Additionally, modern stock assessment methods often allow for ageing error, and the results of this study provide the bases for quantifying this error. The traditional process of preparing skate vertebrae for age determination is very time-consuming and cost prohibitive, and the FT-NIRS approach provides considerable efficiencies. On average it takes 40 minutes to prepare and age one vertebra via traditional methods, while it takes just 5 minutes using FT-NIRS once the calibration model is established. However, it is important to note that the accuracy of FT-NIRS estimates is reliant on the accuracy of the age estimates used to calibrate the predictive model between spectra and age. Longnose Skates have validated annual band periodicity, which made them an ideal candidate for this study (King et al. 2017). The applicability of this technology to other elasmobranchs and batoids will depend on the continuation of rigorous age validation studies for each species (Natanson et al. 2018, Campana 2001).

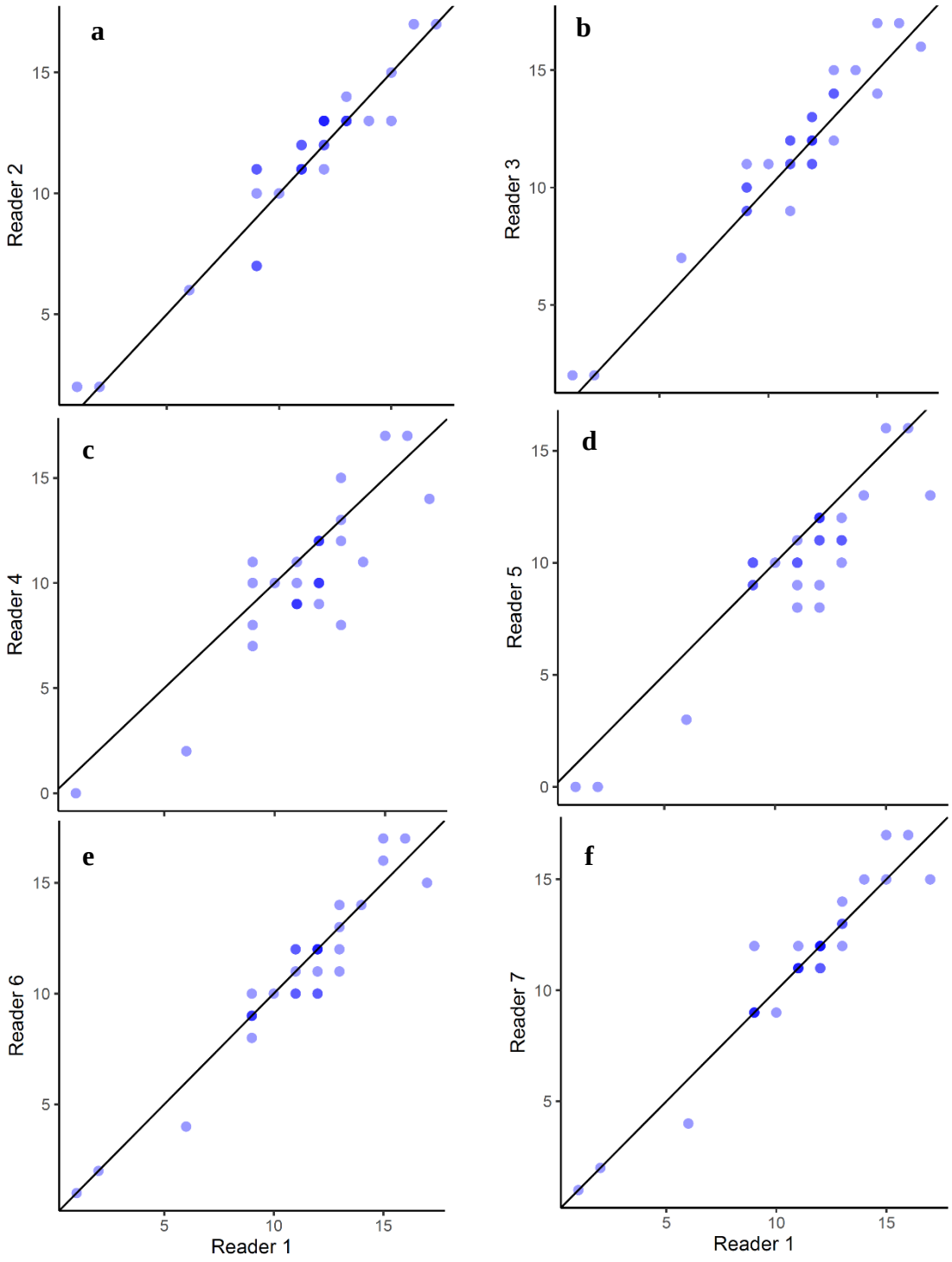

Figure 2.1. Age estimate comparisons between the primary age reader (Reader 1) and readers at a-b) the Alaska fisheries science center c-d) Department of Fisheries and Oceans Canada, and e-f) the Northwest Fisheries Science Center. The black line is the 1-1 line. Age estimates between Reader 1 and Readers 5 and 6 were the least precise. Point shading represents relative sample size.

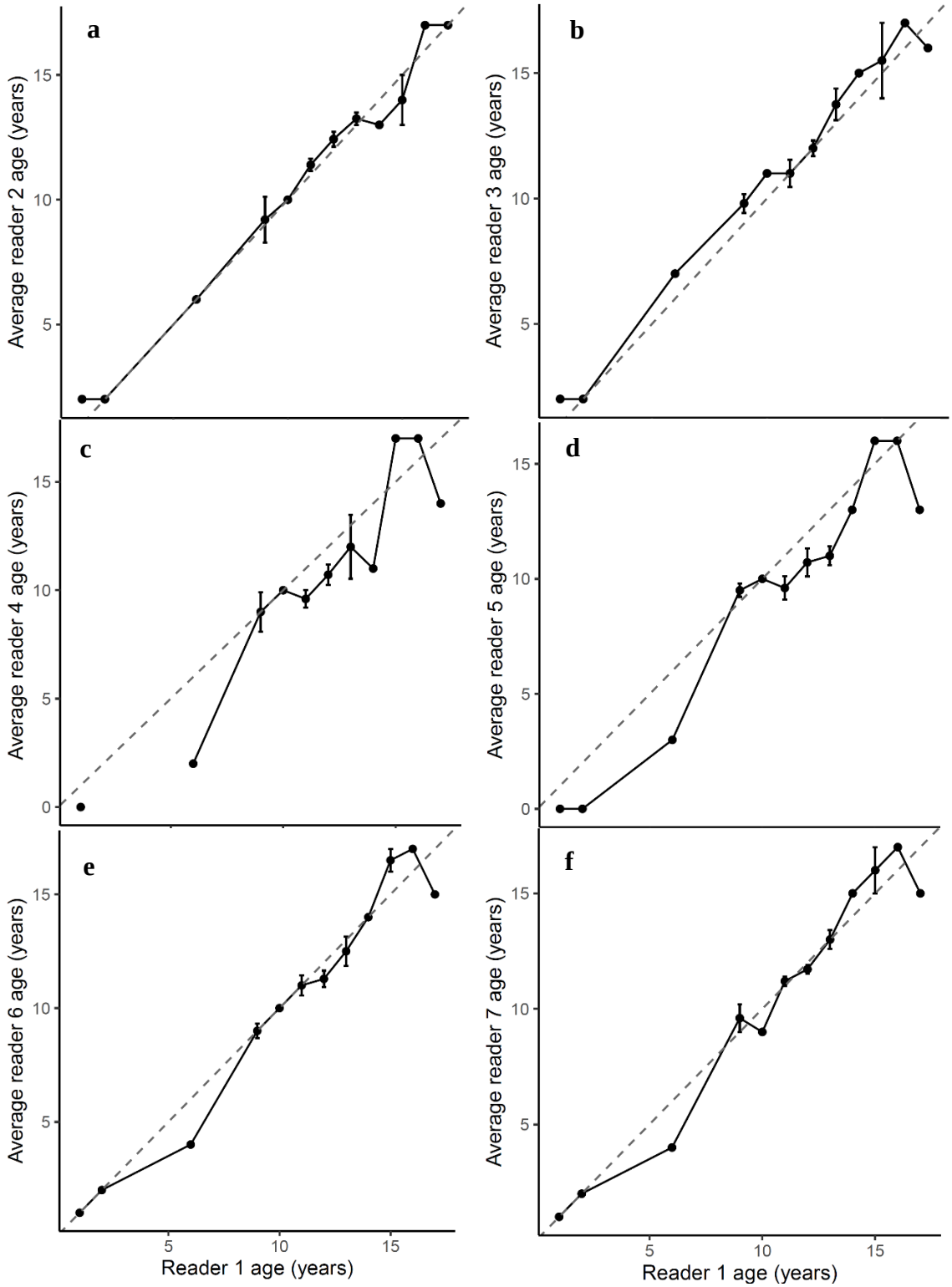

Figure 2.2. Bias plot comparing primary reader (reader 1) estimates to average estimates from age readers at a-b) the AFSC, b-c) DFO, and d-e) the NWFSC. Standard error bars shown for age groups with multiple samples. Bias was most pronounced between the primary reader and age readers from DFO who had a tendency to underage relative to reader 1. Dashed line represents 1:1 agreement between readers.

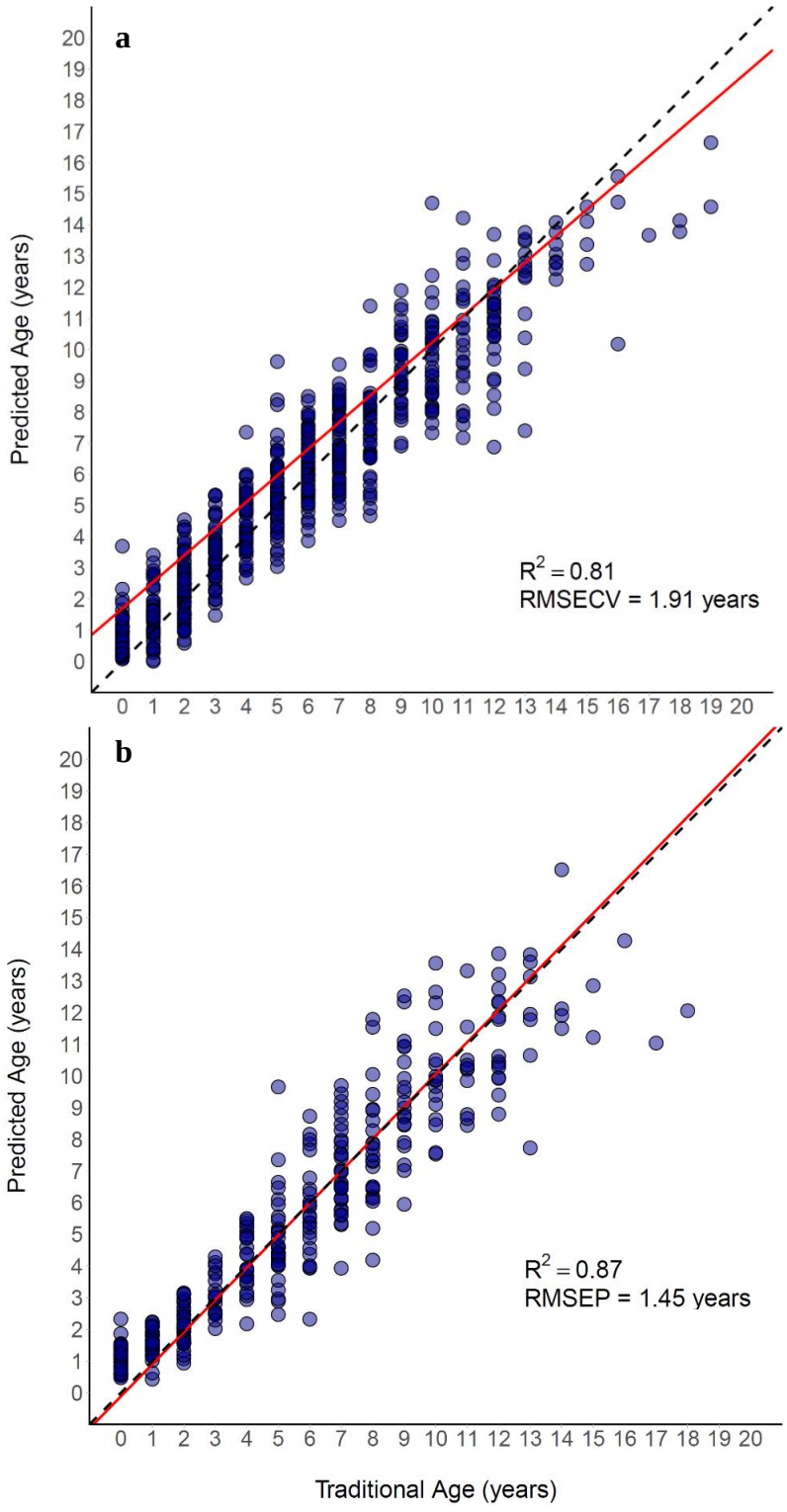

Figure 2.3. Traditionally estimated ages and corresponding predictions from the PLS model predicting age based on near infrared spectra for a) the leave-one-out cross validation and b) external validation. Point shading represents relative sample size.

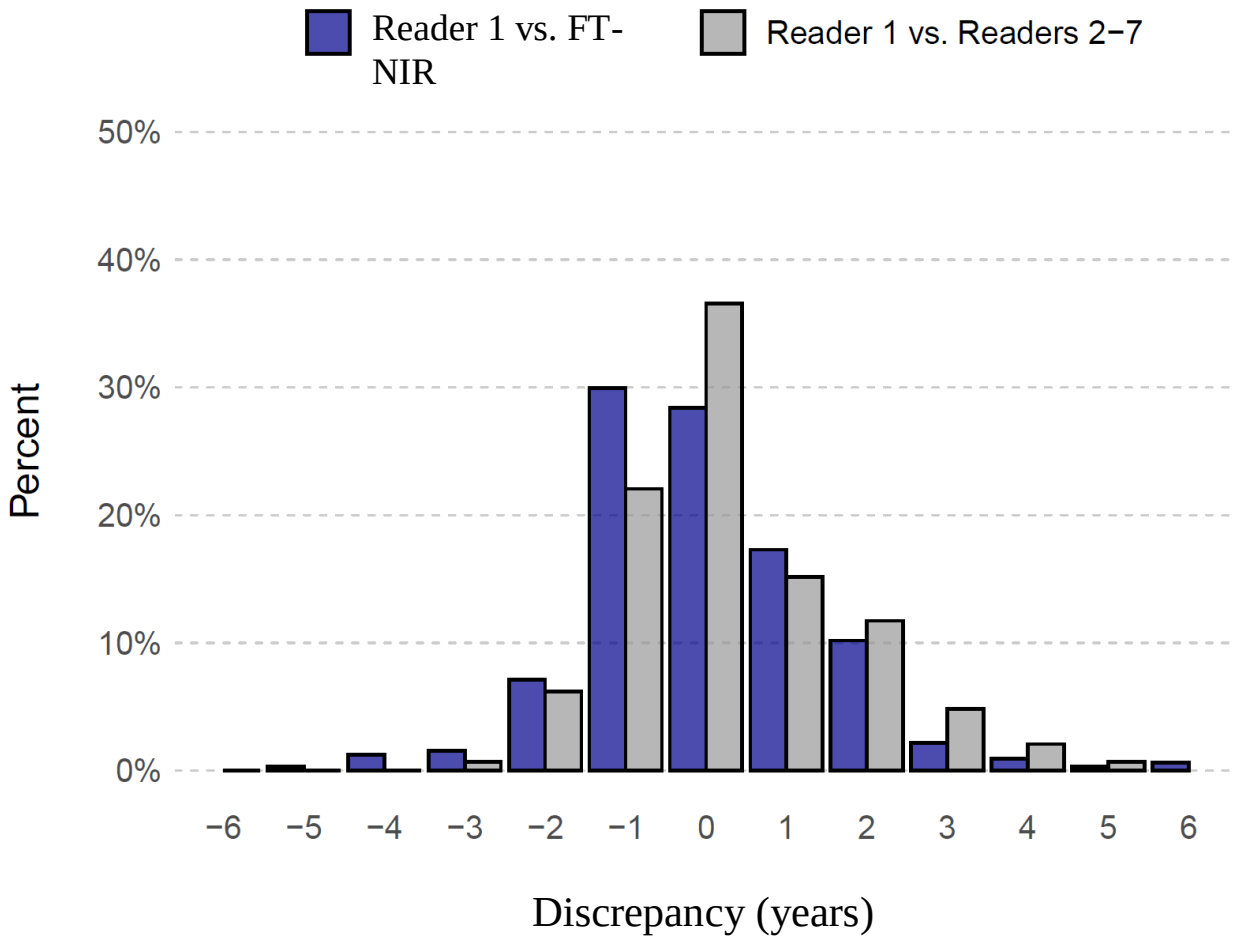

Figure 2.4. Comparing bias in FT-NIRS age estimates to between-age reader bias. Bias shown as percent of specimens with age estimate differences of 0 to 6 years. In blue: Traditional age estimated by reader 1 – FT-NIRS prediction, and in grey: reader 1 – age readers 2-7 from the AFSC, DFO, and NWFSC.

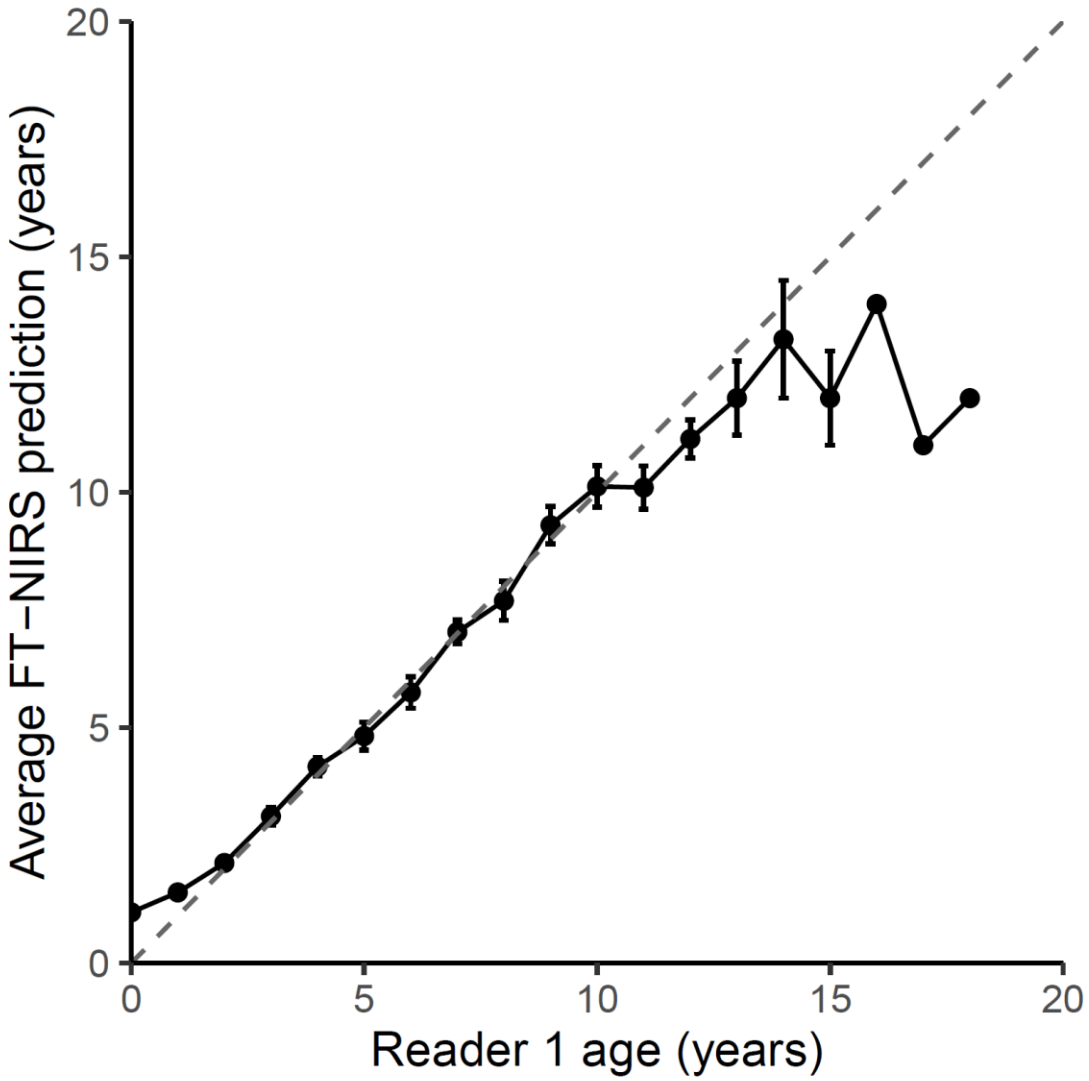

Figure 2.5. Bias plot comparing reader 1) age estimates to average FT-NIRS predictions for each age group. Standard error bars shown for age groups with multiple samples. FT-NIRS predictions had a positive bias relative to the primary reader for young ages (< 2 years) and negative bias for ages over 10 years, but especially for ages 15 and over.

BIBLIOGRAPHY

Adams, G.D., Leaf, R.T., Ballenger, J.C., Arnott, S.A. and C.J. McDonough. 2018. Spatial variability in the growth of Sheepshead (*Archosargus probatocephalus*) in the Southeast US: Implications for assessment and management. Fisheries Research 206: 35–43.

Atkinson, D. and R.M. Sibly. 1997. Why are organisms usually bigger in colder environments? Making sense of a life history puzzle. Trends in Ecology and Evolution 12: 235 – 239.

Barnett, L.A.K., Winton, M.V., Ainsley, S.M., Cailliet, G.M. and D.A. Ebert. 2013. Comparative demography of skates: life-history correlates of productivity and implications for management. PLoS ONE 8, e65000.

Beacham, T.D. 1987. Variation in length and age at sexual maturity of Atlantic groundfish: a reply. Environmental Biology of Fishes 19: 149–153.

Burnham, K.P. and D.R. Anderson. 2002. Model selection and multimodel inference: a practical.

Cailliet, G. M., Smith, W. D., Mollet, H. F. and K.J. Goldman. 2006. Age and growth studies of chondrichthyan fishes: the need for consistency in terminology, verification, validation, and growth function fitting. Environmental Biology of Fishes 77: 211–228.

Campana, S. E. 2001. Accuracy, precision and quality control in age determination, including a review of the use and abuse of age validation methods. Journal of Fish Biology 59: 197–242.

Campana, S.E. 2014. Age Determination of Elasmobranchs, with Special Reference to Mediterranean Species: A Technical Manual. *Food and Agriculture Organization of the United Nations: General Fisheries Commission for the Mediterranean.*

Carlson, J. K. and G.R. Parsons. 1997. Age and growth of the bonnethead shark, *Sphyrna tiburo*, from northwest Florida, with comments on clinal variation. Environmental Biology of Fishes 50: 331–341.

Cavanagh, R.D., M. Camhi, G.H. Burgess, G.M. Cailliet, S.V. Fordham, Colin A. Simpfendorfer, and J.A. Musick. 2005. Sharks, Rays and Chimaeras: The Status of the Chondrichthyan Fishes. Edited by Sarah L. Folwer. IUCN.

Chang, W.Y.B. 1982. A Statistical Method for Evaluating the Reproducibility of Age Determination. Can. J. Fish. Aquat. Sci. 39: 1208–1210.

Chen, J., and X.Z. Wang. 2001. A new approach to near-infrared spectral data analysis using independent component analysis. J. Chem. Inf. Comput. Sci. 41: 992–1001.

Conover, D.O., Brown, J.J. and A. Ehtisham. 1997. Countergradient variation in growth of young striped bass (*Morone saxatilis*) from different latitudes 1. Canadian Journal of Fisheries and Aquatic Sciences 54: 2401–2409.

Davis, C.D., Cailliet, G.M. and D.A. Ebert. 2007. Age and growth of the roughtail skate *Bathyraja trachura* (Gilbert 1892) from the eastern North Pacific. Environ Biol Fish 80: 325–336.

Doll, J. C. and Lauer, T. E. 2013. Bayesian Estimation of Age and Length at 50% Maturity. Transactions of the American Fisheries Society 142: 1012–1024.

Dulvy, N.K., Fowler, S.L., Musick, J.A., Cavanagh, R.D., Kyne, P.M., Harrison, L.R., Carlson, J.K., Davidson, L., Fordham, S.V., Francis, M.P., Pollock, C.M., Simpfendorfer, C.A., Burgess, G.H., Carpenter, K.E., Compagno, L., Ebert, D.A., Gibson, C., Heupel, M.R, Livingstone, S.R., Sanciangco, J.C., Stevens, J.D., Valenti, S. and W. T. White. 2014. Extinction risk and conservation of the world's sharks and rays. eLife 3: 1 – 34.

Ebert, D.A., Smith, W.D. and G.M. Cailliet. 2008. Reproductive biology of two commercially exploited skates, *Raja binoculata* and *R. rhina*, in the western Gulf of Alaska. Fisheries Research 94, 48–57.

Fahy, D.P., Spieler, R.E. and W.C. Hamlett. 2007. Preliminary observations on the reproductive cycle and uterine fecundity of the yellow stingray, *Urobatis jamaicensis* (Elasmobranchii: Myliobatiformes: Urolophidae) in southeast Florida, U.S.A. The Raffles Bulletin of Zoology 14, 131-139.

Gburski, C.M., Gaichas, S.K. and D.K. Kimura. 2007. Age and growth of big skate (*Raja binoculata)* and longnose skate (*R. rhina*) in the Gulf of Alaska. Environmental Biology of Fishes 80: 337–349.

Green, B.S. 2008. Chapter 1 Maternal Effects in Fish Populations. Advances in Marine Biology 54: 1–105.

Gertseva, V., Matson, S. E., Taylor, I., Bizzarro, J. and J. Wallace. 2019. Stock assessment of the Longnose Skate (*Beringraja rhina*) in state and Federal waters off California, Oregon and Washington.

Gertseva, V. V. and M.J. Schirripa. 2007. Status of the Longnose Skate (*Raja rhina*).

Gertseva, V., Matson, S. E. and J. Cope. 2017. Spatial growth variability in marine fish: example from Northeast Pacific groundfish. ICES Journal 74: 1602 – 1613.

Heino, M., Dieckmann, U. and O.R. GODø. 2002. Measuring Probabilistic Reaction Norms for Age and Size at Maturation. Evolution 56: 669–678.

Heino, M. and U. Dieckmann. 2008. Detecting Fisheries-Induced Life-History Evolution: An Overview of the Reaction-Norm Approach. Bulletin of Marine Science 83: 69 – 93.

Helser, T. E., Benson, I., Erickson, J., Healy, J., Kastelle, C., and J.A. Short. 2018. A transformative approach to ageing fish otoliths using Fourier transform near infrared spectroscopy: a case study of eastern Bering Sea walleye pollock (*Gadus chalcogrammus*). Canadian Journal of Fisheries and Aquatic Sciences 1–10.

Kimura, D.K., and D.M. Anderl. 2005. Quality Control of Age Data at the Alaska Fisheries Science Center. Marine and Freshwater Research 56, 5: 783.

King, J.R., Surry, A.M., Garcia, S. and P.J. Starr. Big Skate (*Raja binoculata*) and Longnose Skate (*R. rhina*) stock assessments for British Columbia.

King, J.R., T. Helser, C. Gburski, D.A. Ebert, G. Cailliet, and C.R. Kastelle. 2017. Bomb Radiocarbon Analyses Validate and Inform Age Determination of Longnose Skate (*Raja rhina*) and Big Skate (*Beringraja binoculata*) in the North Pacific Ocean. Fisheries Research 193: 195–206.

Lai, H.L. and D.R. Gunderson. 1987. Effects of ageing errors on estimates of growth, mortality and yield per recruit for walleye pollock (Theragra chalcogramma). Fisheries Research 5, 287–302.

Lorenzen, K. and K. Enberg. 2002. Density-dependent growth as a key mechanism in the regulation of fish populations: evidence from among-population comparisons. Proc Biol Sci 269: 49–54.

Mangel, M. 2017. The inverse life-history problem, size-dependent mortality and two extensions of results of Holt and Beverton. Fish and Fisheries 18: 1192–1200.

Matta, M.E., and D.R. Gunderson. 2007. Age, Growth, Maturity, and Mortality of the Alaska Skate, *Bathyraja Parmifera*, in the Eastern Bering Sea. Environmental Biology of Fishes 80: 309 – 323.

Matta, M.E., Black, B.A., and T.K. Wilderbuer. 2010. Climate-driven synchrony in otolith growth-increment chronologies for three Bering Sea flatfish species. Mar Ecol Prog Ser 413:137–145.

Matta, M.E., Tribuzio, C.A., Ebert, D.A., Goldman, K.J., and C.M. Gburski. 2017. Age and Growth of Elasmobranchs and Applications to Fisheries Management and Conservation in the Northeast Pacific Ocean. In Advances in Marine Biology, 77:179–220. Elsevier, 2017.

Matta, M. E., Helser, T. E., and B.A. Black. 2018. Intrinsic and environmental drivers of growth in an Alaskan rockfish: an otolith biochronology approach. Environmental Biology of Fishes 101: 1571–1587.

Matta, M. E., Rand, K.M., Arrington, M.B., and B.A. Black. 2020. Competition-driven growth of Atka mackerel in the Aleutian Islands ecosystem revealed by an otolith biochronology. Estuarine, Coastal and Shelf Science. In Review.

Maunder, M.N., Crone, P.R., Valero, J.L., and B.X. Semmens. 2015. Growth: Theory, Estimation, and Application in Fishery Stock Assessment Models CAPAM Workshop Series Report 2. Center for the Advancement of Population Assessment Methodology (CAPAM), NOAA/IATTC/SIO, 8901 La Jolla Shores Dr., La Jolla, 92037, CA, http://www.capamresearch.org/growth/workshop 55 p.

McBride, R. S. 2015. Diagnosis of paired age agreement: a simulation of accuracy and precision effects. ICES Journal of Marine Science. 72: 2149–2167.

McClure, W., Crowell, B., Stanfield, D., Mohapatra, S., Morimoto, S., and G. Batten. 2002. Near infrared technology for precision environmental measurements: Part1. Determination of nitrogen in green-and dry-grass tissue. J. Near Infrared Spectrosc. 10: 177–185.

McFarlane, G.A. and J.R. King. 2006. Age and Growth of Big Skate (*Raja binoculata*) and Longnose Skate (*Raja rhina*) in British Columbia Waters. Fisheries Research 78: 169–78.

Mello, L.G.S. and G.A. Rose. 2005. Seasonal growth of Atlantic cod: effects of temperature, feeding and reproduction. Journal of Fish Biology 67: 149–170.

Morita, K. and S.H. Morita. 2002. Rule of age and size at maturity: individual variation in the maturation history of resident white-spotted charr. Journal of Fish Biology 61: 1230–1238.

Natanson, L. J., Skomal, G. B., Hoffman, S. L., Porter, M. E., Goldman, K. J., and D. Serra. 2018. Age and growth of sharks: do vertebral band pairs record age? Marine Freshwater Research 69: 1440.

Ormseth, O. A. 2017. Assessment of the skate stock complex in the Gulf of Alaska. NPFMC Gulf of Alaska SAFE 223 – 280.

Pardo, S.A., Cooper, A.B. and N.K. Dulvy. 2013. Avoiding fishy growth curves. Methods in Ecology and Evolution 4: 353–360.

Reum, J. C. P., Essington, T. E., Greene, C. M., Rice, C. A., Polte, P., and K.L. Fresh. 2013. Biotic and abiotic controls on body size during critical life history stages of a pelagic fish, Pacific herring (*Clupea pallasii*). Fisheries Oceanography 22, 324–336.

Rigby, C. L., B. B. Wedding, S. Grauf, and C. A. Simpfendorfer. 2016. Novel Method for Shark Age Estimation Using near Infrared Spectroscopy. Marine and Freshwater Research 67, 5: 537.

Robins J.B., B.B. Wedding, C. Wright S. Grauf, M. Sellin, A. Fowler, T. Saunders, and S. Newman. 2015. Department of Agriculture, Fisheries and Forestry, Revolutionising Fish Ageing: Using Near Infrared Spectroscopy to Age Fish.

Roff, D. A. 1991. The evolution of life-history variation in fishes, with particular reference to flatfishes. Netherlands Journal of Sea Research 27, 197–207.

Roggo Y., Chalus, P., Maurer, L., Lema-Martinez, C., Edmond, A. and N. Jent. 2007. A review of near infrared spectroscopy and chemometrics in pharmaceutical technologies. J. Pharm. Biomed. Anal. 44: 683–700.

Shelton, A. O. and M. Mangel. 2012. Estimating von Bertalanffy parameters with individual and environmental variations in growth. Journal of Biological Dynamics 6: 3–30.

Stawitz, C. Understanding the Effects of Growth and Size-at-Age Variation on the Dynamics of Fish Populations. (University of Washington, 2017).

Stawitz, C. C. and T.E. Essington. 2019. Somatic growth contributes to population variation in marine fishes. Journal of Animal Ecology 88: 315–329

Stearns, S. C. 1992. The Evolution of Life Histories. Oxford: Oxford University Press.

Stokes, K. and R. Law. 2000. Fishing as an evolutionary force. Mar. Ecol. Prog. Ser. 208:307–309.

Thompson, J.E. 2005. Age, Growth and Maturity of the Longnose Skate (*Raja rhina*) for the US West Coast and Sensitivity to Fishing Impacts MS Thesis. State University, Oregon.

Tuckey, T., Yochum, N., Hoenig, J., Lucy, J. and J. Cimino. 2007. Evaluating Localized vs. Large-scale Management: The Example of Tautog in Virginia. Fisheries 32, 21–28.

Vitale, F., Svedäng, H. and M. Cardinale. 2006. Histological analysis invalidates macroscopically determined maturity ogives of the Kattegat cod (*Gadus morhua*) and suggests new proxies for estimating maturity status of individual fish. ICES Journal Marine Science 63: 485–492.

von Bertalanffy, L. 1957. Quantitative Laws in Metabolism and Growth. The Quarterly Review of Biology 32: 217–231.

Wedding, B.B., Forrest, A.J., Wright, C., Grauf, S., and P. Exley. 2014. A novel method for the age estimation of saddletail snapper (*Lutjanus malabaricus*) using Fourier transform – near infrared (FT-NIR) spectroscopy. Mar. Freshw. Res. 65: 894–900.

Williams, B.C., Kruse, G.H. and M.W. Dorn. 2016. Interannual and Spatial Variability in Maturity of Walleye Pollock *Gadus chalcogrammus* and Implications for Spawning Stock Biomass Estimates in the Gulf of Alaska. PLoS One; San Francisco 11.

Zeiner, S.J. and P. Wolf. 1993. Growth characteristics and estimates of age at maturity of two species of skates (*Raja binoculata and Raja rhina*) from Monterey Bay, California. US Dept Commer NOAA Tech Rep 115: 87–99.